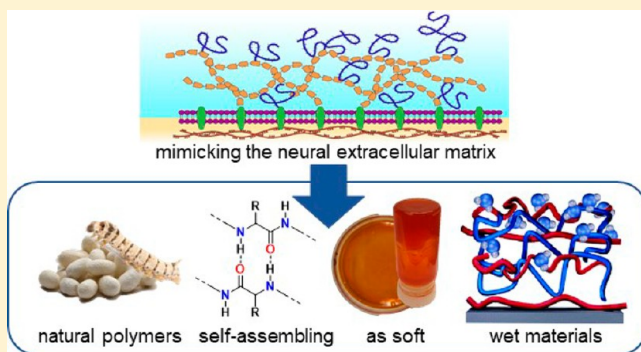


# Layers and Multilayers of Self-Assembled Polymers: Tunable Engineered Extracellular Matrix Coatings for Neural Cell Growth

Michael J. Landry,<sup>†</sup> Frédéric-Guillaume Rollet,<sup>†</sup> Timothy E. Kennedy,<sup>\*,‡</sup> and Christopher J. Barrett<sup>\*,†</sup>

<sup>†</sup>Department of Chemistry and <sup>‡</sup>Department of Neurology and Neurosurgery, Montreal Neurological Institute and Hospital, McGill University, Montreal, Quebec H3A 0B8, Canada

**ABSTRACT:** Growing primary cells and tissue in long-term cultures, such as primary neural cell culture, presents many challenges. A critical component of any environment that supports neural cell growth *in vivo* is an appropriate 2-D surface or 3-D scaffold, typically in the form of a thin polymer layer that coats an underlying plastic or glass substrate and aims to mimic critical aspects of the extracellular matrix. A fundamental challenge to mimicking a hydrophilic, soft natural cell environment is that materials with these properties are typically fragile and are difficult to adhere to and stabilize on an underlying plastic or glass cell culture substrate. In this review, we highlight the current state of the art and overview recent developments of new artificial extracellular matrix (ECM) surfaces for *in vitro* neural cell culture. Notably, these materials aim to strike a balance between being hydrophilic and soft while also being thick, stable, robust, and bound well to the underlying surface to provide an effective surface to support long-term cell growth. We focus on improved surface and scaffold coating systems that can mimic the natural physicochemical properties that enhance neuronal survival and growth, applied as soft hydrophilic polymer coatings for both *in vitro* cell culture and for implantable neural probes and 3-D matrixes that aim to enhance stability and longevity to promote neural biocompatibility *in vivo*. With respect to future developments, we outline four emerging principles that serve to guide the development of polymer assemblies that function well as artificial ECMs: (a) design inspired by biological systems and (b) the employment of principles of aqueous soft bonding and self-assembly to achieve (c) a high-water-content gel-like coating that is stable over time in a biological environment and possesses (d) a low modulus to more closely mimic soft, compliant real biological tissue. We then highlight two emerging classes of thick material coatings that have successfully captured these guiding principles: layer-by-layer deposited water-soluble polymers (LbL) and silk fibroin (SF) materials. Both materials can be deposited from aqueous solution yet transition to a water-insoluble coating for long-term stability while retaining a softness and water content similar to those of biological materials. These materials hold great promise as next-generation biocompatible coatings for tissue engineers and for chemists and biologists within the biomedical field.



## INTRODUCTION

For over 100 years, researchers have employed *in vitro* cell culture methods to study neural cells; however, the artificial substrates and matrices typically used to maintain cell survival and differentiation provide a relatively poor approximation of biological tissue. Artificial polymer coatings are relatively inexpensive, stable, and straightforward to prepare yet typically provide a poor approximation of real soft and wet biological tissue and thus often perform suboptimally. A bare polystyrene plastic surface, for example, generally will not support living cells, and most thin polymer coatings, which are similarly hydrophobic and brittle, will not significantly extend cell viability. While systems that incorporate natural biosourced polymers have been developed, these are typically not stable over weeks, are difficult to work with, or are prohibitively expensive to purchase or manufacture in bulk. Poly-L-lysine (PLL), a homopolymer of the naturally occurring amino acid L-lysine, has long dominated the field as the gold standard; however, it is readily degraded by cellular proteases. The application of its mirror twin poly-D-lysine

(PDL) displays similar efficacy yet is more resistant to proteolytic degradation than PLL. Advances in molecular biology have identified key components of the extracellular matrix (ECM) that critically support cell survival, differentiation, and growth *in vivo*. Recent studies aim to capture the properties of natural ECM that enhance neuronal survival and growth using novel soft-water-soluble polymers to coat substrates for neural cell culture, implantable neural electrodes and probes, and 3-D matrixes to enhance stability *in vivo* and increase neural biocompatibility. Here, we review recent advancements in the development of improved surface and scaffold coatings that employ principals of biomimicry at the molecular scale, with the ultimate goal of engineering a thick, soft, and wet transformative neural interface.

**Received:** November 30, 2017

**Revised:** February 24, 2018

**Published:** February 26, 2018

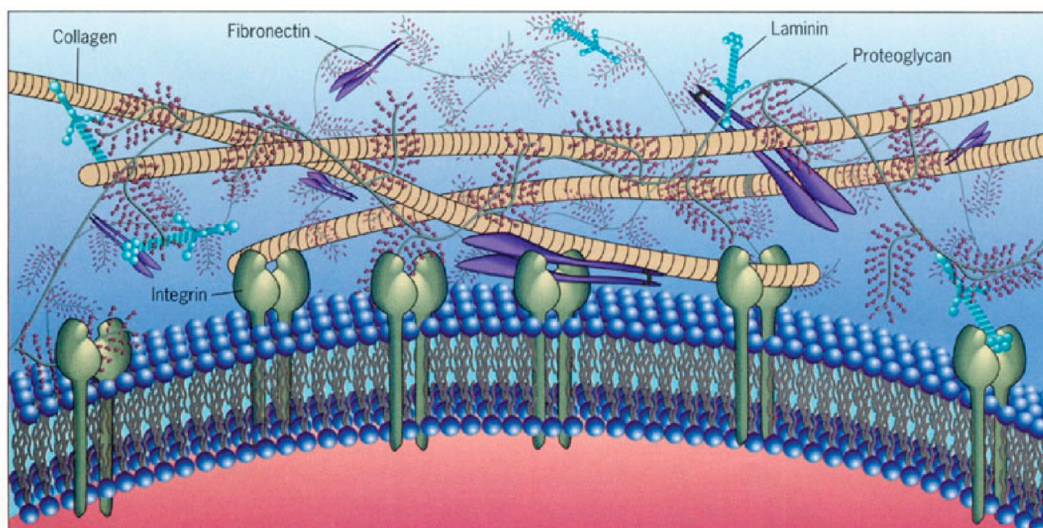


**Figure 1.** Schematic of the various components of ECM. Integrins bind extracellular proteins, such as collagen fibers decorated with proteoglycans. The specific proteins and glycans present differentiate ECMs found in different tissue types. Transmembrane integrin proteins are linked on the cytosolic side of the plasma membrane phospholipid bilayer to cytoskeletal elements, such as microfilaments composed of filamentous actin, intermediate filaments, and microtubules composed of polymerized tubulin. By linking the intracellular cytoskeleton to the local ECM, integrins transduce force across the plasma membrane. Adapted from Karp et al.<sup>9</sup> with permission from John Wiley and Sons, “Cell and Molecular Biology: Concepts and Experiments”, 4th ed. Copyright 2006.

## ■ BACKGROUND

The extracellular matrix (ECM) is a cell-type and tissue-specific organized array of proteins and polysaccharides secreted by cells that define the molecular composition of the local environment and provide structural and biochemical support.<sup>1</sup> These macromolecular assemblies typically closely associate with cell surfaces, with some components binding directly to transmembrane receptors (Figure 1). Integrins, a key family of receptors, mediate cell adhesion via specific interactions with major ECM components that include members of the fibronectin, vitronectin, collagen, and laminin protein families. Upon ligand binding, integrins initiate intracellular signal cascades that regulate the organization of the cytoskeleton, cell migration, the formation of specialized adhesive junctions, and the trafficking of secretory proteins and receptors to the plasma membrane.<sup>1,2</sup> Laminin superfamily members are core components of basal lamina ECM and are often employed in neuronal cell culture as a substrate to promote cell migration, adhesion, and neurite extension.<sup>1</sup> Fibronectin exists as either soluble plasma fibronectin or insoluble cellular fibronectin and influences cell adhesion, growth, differentiation, wound healing, embryonic development, and migration.<sup>1</sup> Although the molecular composition of the ECM is complex, and cell- and tissue-specific, synthetic ECM replacements have been used to support cell growth in vitro for many years.<sup>3</sup> The coatings produced by manufacturers are frequently proprietary, and their exact compositions often remain trade secrets. With recent advancements in tissue engineering, ECM replacements have moved increasingly from two-dimensional films to three-dimensional scaffolds, with polymer chemists, cell biologists, and materials engineers working together to design materials that more realistically mimic tissue environments. The development of specialized materials to support three-dimensional artificial ECM presents an opportunity to create mimics of neuronal tissue that support the formation of three-dimensional networks of neurons and glial cells. Naturally derived polymers such as hyaluronic acid (HA), a major component of the ECM in the central nervous

system (CNS),<sup>4,5</sup> have been employed with the promise of improving the neuronal cell culture, along with fibrous polymers such as collagen, fibronectin, and elastin.<sup>6,7</sup> However, these relatively large proteins are expensive and fragile and can be difficult to prepare and store while maintaining their biological activity, compared to synthetic counterparts, and there has been relatively little research into chemical modifications to enhance their stability and ease of use. While the biochemical–structural components of the ECM are complex, simple mimics of their basic mechanical and biochemical properties have been proposed in a variety of systems.<sup>3,8</sup> Critical features of materials that aim to mimic the ECM can be summarized by two guiding principles (self-assembly and biomimicry) and two key material properties (low modulus and high water content).

**Specific Requirements of Neural Cells.** Neurons are highly specialized cells that are critical to sensation, movement, and cognition.<sup>10</sup> Loss of neurons and deficient neuronal function underlie neurodegenerative disorders such as Alzheimer’s and Parkinson’s diseases.<sup>11</sup> Developing materials that support neural growth and enhance neural biocompatibility may ultimately find utility in the treatment of neurodegenerative disease. Such materials will also facilitate the study of neural cells. Historically, neurons have been cultured on surfaces that attempted to capture and mimic critical physical or chemical aspects of a real ECM. During the first decade of the 20th century, the first experiments to visualize living neurons in cell culture utilized glass coverslips and a microscope, combined with a technique pioneered by Ross Granville Harrison called a hanging drop, a technique that examined fragments of the embryonic nervous system within a liquid drop hanging from a sterile coverslip inverted on a watch glass.<sup>12</sup> This technique allowed for small explants of living tissue to be viewed in three dimensions rather than two. The neurons quickly died, however, due to the absence of adequate access to nutrition and mechanical support. At the time, it was not clear if the elaboration of a process by a neuron required a substrate or alternatively if neurons might extend processes like a tree extends branches into the air. To determine

if mechanical support is required, Harrison conducted a series of experiments using spider silk as a substrate for neural cell culture. Fibrous substrates were generated by having spiders spin a web at the bottom of a jar, and once finished, tissue explants from embryonic chick or frog CNS were placed on top (Figure 2A,B).<sup>13</sup> Processes from the excised tissue were observed

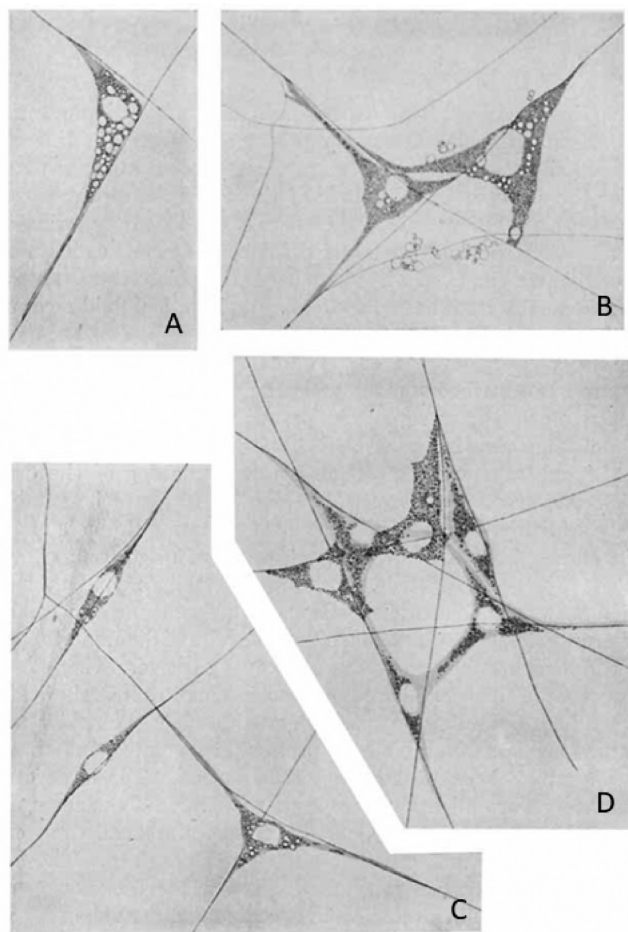


**Figure 2.** Illustrations from Harrison's pioneering paper titled "The reaction of embryonic cells to solid structures" which demonstrates some of the first uses of artificial substrates for the cultivation of neural cells. (A) Cells from an explant of an embryonic frog CNS are cultured with serum on crossed spider webs (300 $\times$ ). Bipolar and tripolar cells from a medullary cord are attached to crossed webs at (B) 8 and (C) 2 days (both 300 $\times$ ). (D) Drawing of the cells after 6 days, showing both pigment cell types that Harrison noticed (300 $\times$ ). Reprinted from Harrison et al.<sup>13</sup> with permission from John Wiley and Sons, *J. Exp. Zool.* Copyright 1914.

to extend along the silk fibers, providing the first experimental evidence that neural cells utilize a mechanical substrate to extend processes.<sup>13</sup> Although not highlighted in these early papers at the time, they represent a foundational application of biomaterials to support the survival and growth of neurons in vitro.

While the vast majority of subsequent studies of neurons in culture have employed one or two layers as a substrate, thicker biomaterial films are currently being explored as coatings to determine the effects of thickness and modulus on the longevity, connectivity, and density of neurons maintained in vitro. Many studies highlight the role of surface stiffness (measured as the modulus, the slope of a stress–strain curve) in neuronal cell survival and the formation of a neural network.<sup>14</sup> An ideal model

system would permit a tunable modulus to allow the cultivation of neuronal (or other) cells in an in vitro environment that is as similar as possible to the specific moduli experienced in vivo, which can vary over a wide range, and to which cells appear to be surprisingly sensitive. Too soft an artificial surface can be just as inappropriate as too hard a surface, and the "goldilocks zone" between them for successful growth appears to be limited to a narrow range of just 20–30% in modulus from an ideal target.<sup>15,16</sup>

**Classes of Materials for Attempted Use as Artificial ECMs.** Systems such as silk fibroin (SF) and layer-by-layer deposited (LbL) polymers, in principle, possess the key characteristic of a tunable modulus, as both can be readily deposited or assembled from aqueous solution yet each becomes adhered, stable, and insoluble while retaining soft gel-like properties that resemble those of a real ECM, to a controllable extent. Key to both systems is a complex substructure composed of soft bonds that assemble during or following deposition, folding up into  $\beta$ -sheets in the case of SF<sup>17</sup> and pairing into ionically bonded multiple layers in the case of LbL, the degree to which can be controlled precisely during fabrication to influence both the water content and the modulus.<sup>18</sup> Silk is a naturally derived and complex material which, while more traditionally challenging to work with, has recently been making important inroads into the biomaterial and biomedical fields. LbL is an assembly technique that can be employed to construct multicomponent systems of simple artificial and/or natural polyelectrolytes, including silk.

Silk fibroin from *Bombyx mori* silk worms is a polypeptide chain consisting of several domain-specific sequences of amino acids that is carefully wound, as a single extruded filament, into a cocoon in preparation for metamorphosis in the *B. mori*'s lifecycle. Compared to other polymers found to possess excellent properties as ECMs for neurons, SF is inexpensive and relatively easy to process and is found to perform at least as well as PDL/PLL, a standard substrate for neuronal culture,<sup>19</sup> largely due to SF's soft modulus and tunability. Layer-by-layer polymer deposition can be used to build up self-assembled polymer coatings onto substrates through electrostatic interactions by alternating polyanionic and polycationic polymers. The loop length between attachment points and thus the ability to hold water and the softness can be tuned precisely by the conditions of chemical deposition, such as ionic strength and pH, in the dipping assembly baths. The influence of the coating modulus on neuronal cells in culture has been well studied, with the general conclusion emerging that neurons grow best on softer materials, up to a specific maximal softness.<sup>20,21</sup> A thin layer of PLL on glass or plastic might serve to mask the hard SiO<sub>2</sub> or polystyrene surface chemically, yet the stiffness of such thin coatings generally still resembles that of the underlying hard support material. This stiffness is typically many MPa (the slope of indentation vs force), which can be a million or more times harder than the stiffness of living neural tissue, which is in the range of 10–100 Pa.<sup>22</sup> The key concept of modulus matching is to grow cells on surfaces and scaffolds that are as similar in modulus as possible to the native tissue.<sup>23,24</sup>

While increasing evidence indicates that relatively low modulus materials generate better neuronal culture conditions, the water content is a critical factor as well, though it is more challenging to obtain accurate measurements of the water content to guide the development of enhanced cell culture substrates.<sup>24,25</sup> Another reason why the modulus has been targeted to guide new material development is the stark disparity

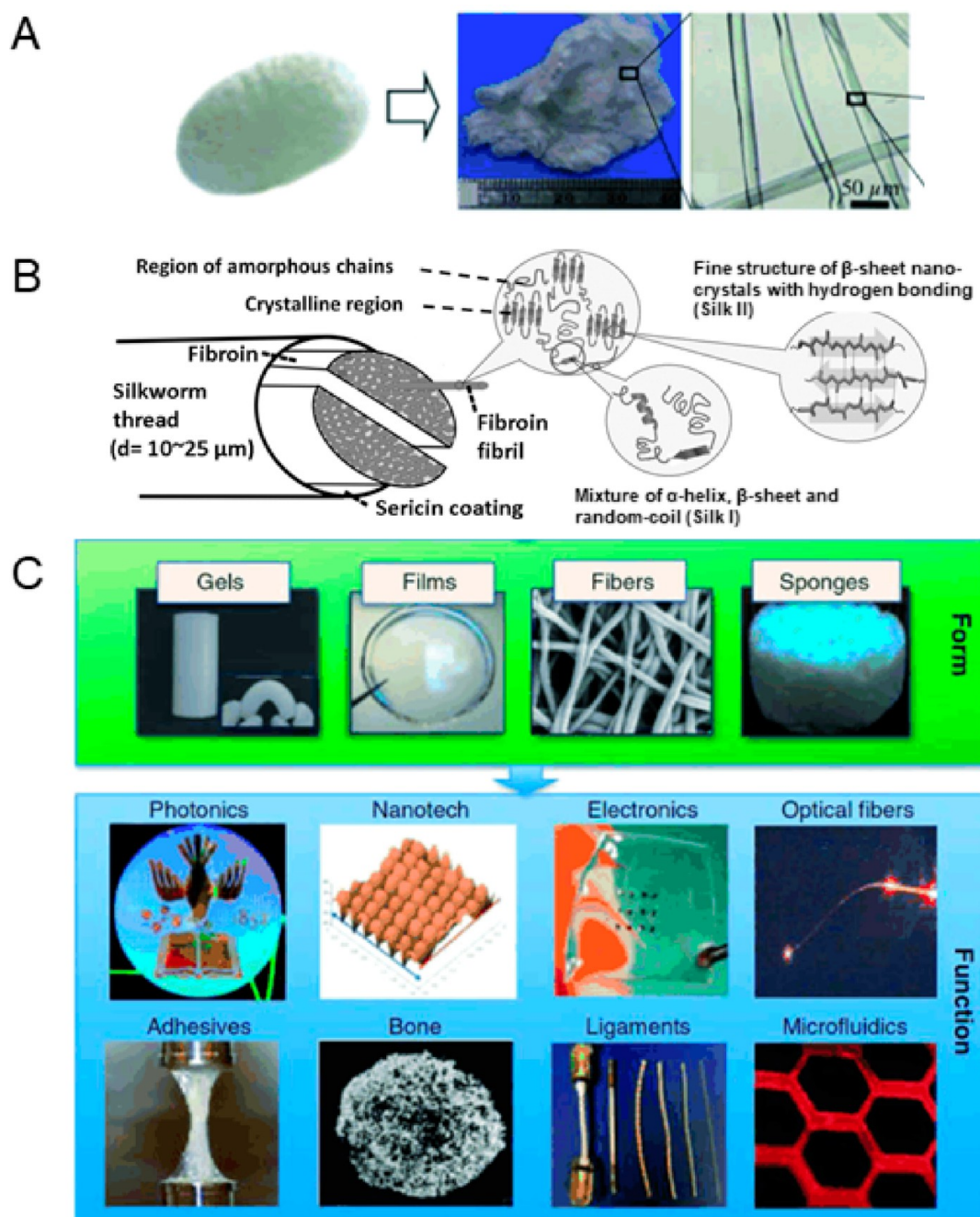


**Figure 3.** (A, left) Cocoon from a *B. mori* silk worm during metamorphosis. (A, right) Resulting material after degumming the silk cocoons and removing the sericin coating and a light microscope image of the resulting bundled fibers after the removal of sericin. (B) Schematic representation of the components comprising silk fibers. A bundle of fibers ( $d = 10\text{--}25\ \mu\text{m}$ ) is surrounded with a coating of sericin. Fibroin contains multiple fibroin fibrils which have distinct packing motifs, including amorphous chains, silk I (a mixture of  $\alpha$ -helices,  $\beta$ -sheets, and random coils), and silk II ( $\beta$ -sheet regions making dense crystalline regions). (C) Examples of four different platforms of silk (gels, films, fibers, and sponges) and their corresponding potential applications (in photonics, nanotechnology, electronics, optical fibers, adhesives, bone scaffold materials, ligaments, and microfluidics). Adapted from (A, C) Ghezzi et al.<sup>35</sup> and (B) Volkov et al.<sup>36</sup> with permission from John Wiley and Sons, (A, C) *Isr. J. Chem.*, Copyright 2013, and (B) *Macromol. Mater. Eng.*, Copyright 2015.

between some of the currently best available cell culture materials on the market and real tissue; a difference in water content between real and artificial systems may be just a few tens of percent, while in contrast the stiffness of artificial systems is often mismatched by a factor of a million to that of real tissue.<sup>22</sup> Available high-water-content materials include hydrogels and layer-by-layer (LbL) systems. Both of these techniques afford good control over the final properties during fabrication,

allowing for highly tunable water content and moduli. High-water-content hydrogels have been rationally designed,<sup>26</sup> with upwards of 80% water content obtained in silk fibroin gels.<sup>27</sup> In spite of this, it remains a challenge to maintain the stability of such intrinsically hydrophilic material on a surface, with sufficient stability to limit rearrangement and dissolution. For silk gels, two microstructures are present in equilibrium: blocks of hard, insoluble  $\beta$ -sheets and an amorphous entangled matrix of higher

water content and lower modulus. The balance between the two phases is controlled by the setting or curing time, which governs the stability to redissolution, and also both the modulus and water content. Typically, SF curing is achieved through methanol exposure or water annealing. Each technique allows further tailoring of the material's properties through the treatment time, temperature, or concentration, which can heavily alter the water content and stability of SF-based materials. This inverse relationship between the modulus and stability and the water content typically works in favor of the materials chemist due to the goal of obtaining high-water-content materials with lower moduli. For LbL systems, varying the pH and salt conditions during the deposition of the polyelectrolyte multilayer film can be employed to control the final water content. These films have been shown to have a high water content, while the exact roles of thickness, water content, and modulus have been explored combinatorially via 1-D and 2-D gradient films in LbL systems.<sup>23,28</sup>

Polymers that self-assemble into rationally designed architectures often can be manipulated to possess a low modulus and a high water content. Such systems assemble into a thermodynamic minimum conformation, with a controllable, predictable spatial arrangement on a surface, leading to a stable and reproducible platform for investigating and optimizing cell compatibility. Natural polymers, such as ECM proteins and intracellular cytoskeletal proteins, employ components that self-assemble and exert a profound influence on the modulus and structural integrity of neural tissues. Self-assembled systems characteristically employ hydrogen or ionic "soft" bonding to generate precise yet reversible spatial arrangements of materials, such as the  $\beta$ -sheets in silk. Importantly, these soft bonds are dynamic and can dissociate and rebond depending on the impinging stimuli, creating a dynamic system with the capacity to adapt and self-repair. Ionic bonds have been used to rationally design three-dimensional tailored materials, such as layer-by-layer (LbL) assemblies that interact via electrostatic interactions between successive layers of alternately charged polyelectrolytes. The capacity to engineer systems utilizing the flexibility of hydrogen and ionic bonding provides the potential to generate more complex, rationally designed dynamic molecular architectures.

The fundamental mechanical properties of a polymer provide some insight into how well a material will perform under a stress or load. There are several experiments designed to quantify the maximum extent to which a polymer can be strained, and the linear initial and reversible regions of these stress–strain curves quantify how elastic or soft a material is, measuring a deformation experienced over the application of a force to a specific cross-sectional area of an object and expressed in terms of a force/area such as a Pascal ( $\text{N}/\text{m}^2$ ). Strain is the material's dimensional response to a stress and can be expressed as the percentage increase of a material's extension in the case of tension.<sup>29</sup> The elastic modulus is a measure of a polymer's resistance to being deformed reversibly under stress and is defined as the slope of the stress–strain curve in the elastic low-stress region. Young's modulus describes the uniaxial tensile elasticity and determines how elastic a material behaves under tensile stress, while a bulk modulus (or elastic modulus), perhaps more relevant to cell culture, describes an extension of Young's modulus in three dimensions of elasticity and is typically determined through indentation. ECM components generally possess high tensile strength but a low elastic modulus (i.e., "tough" polymers, typical of natural materials), and these attributes are what functional

artificial ECM materials typically mimic.<sup>30</sup> A majority of biologically derived materials are soft yet tough, such as SF, HA, cellulose, and spider silk. Structure–performance relationships have been studied between the softness of a material and how well it performs as an artificial ECM replacement for growing neuronal cells.<sup>21</sup>

Inspired by cell biology and biochemistry, we envision that an ideal system will possess a tunable modulus and a high water content and will rely on efficient self-assembly. Typically, within natural systems, these guiding principles are highly prevalent, thus we believe that it is important to design artificial systems with these design paradigms in mind. Of all of the various systems currently being studied, silk polymers and LbL systems best fit these specifications. The LbL approach involves layering polycationic and polyanionic polymers in alternating secession to generate multilayered soft-bonded substrates that have much freedom in structure and thus a high water content and low modulus. Both silk gels and LbL coatings have predictably been shown to control both the modulus and water content through a self-assembly process. We present a concise review first of silk-based materials and then of LbL-based materials for growing neuronal cultures.

**Silk as an Artificial ECM Material.** Naturally derived biomaterials have been extensively explored for use in biomedical applications,<sup>31</sup> cell guidance,<sup>32</sup> surface coatings,<sup>4</sup> and biomedical devices.<sup>33</sup> Silk embodies some of the best properties of successful artificial ECM. It is tough, having a high tensile modulus but a low elastic modulus, possesses a high water content, and can be processed into a variety of different forms and geometries.<sup>34</sup> Of all the types of SF being explored, *Bombyx mori* silk fibroin (Figure 3A,B) possesses perhaps the most ideal properties while being a readily available, relatively inexpensive starting material yet possessing a rich suite of material chemistry properties that are highly controllable through processing (Figure 3C).

*Bombyx mori* silk is a fibrous polymer chain of amino acids that possesses two unique structural motifs: well-defined crystalline phases and an irregular amorphous phase in between.<sup>37</sup> The crystalline domain is composed of repeating units of glycine combined with alanine, serine, or tyrosine (Figure 3A,B). These repeating amino acid units produce different polymorphic domains due to different packing motifs: silk I, silk II, and silk III.<sup>37</sup> Silk I is defined as the glandular state, a series of extended  $\alpha$ -helices that are water-soluble.<sup>37</sup> Silk II possess a well-defined  $\beta$ -sheet conformation that is generally water insoluble, and silk III is a 3-fold polyglycine II-like helix that naturally occurs at the water–air interface during the process of spinning.<sup>37</sup> Silk III is the polymorphic form that *B. mori* silk worms excrete during pupation and is generally water-insoluble to protect the growing worm during the process of metamorphosis. Although natural silk is largely composed of silk III, a small amount of the crystalline region is also silk II, allowing the material to be relatively water-impervious yet pliable.<sup>38</sup> Interconversion between silk I and silk II is achieved by gentle heating and exposure to methanol or potassium chloride, producing water-stable films.<sup>38</sup> These films resist redissolution yet present a platform to introduce water reuptake into the film through water swelling, forming the various material classes into which silk can be processed.<sup>39</sup>

In order to process silk into various material forms, an aqueous solution of silk is first required. Natural silk cocoons contain two polymeric components, silk fibroin and sericin, that must be separated prior to solubilizing the fibroin. Silk can be isolated by boiling the cocoons with  $\text{Na}_2\text{CO}_3$ , releasing the native silk fibers

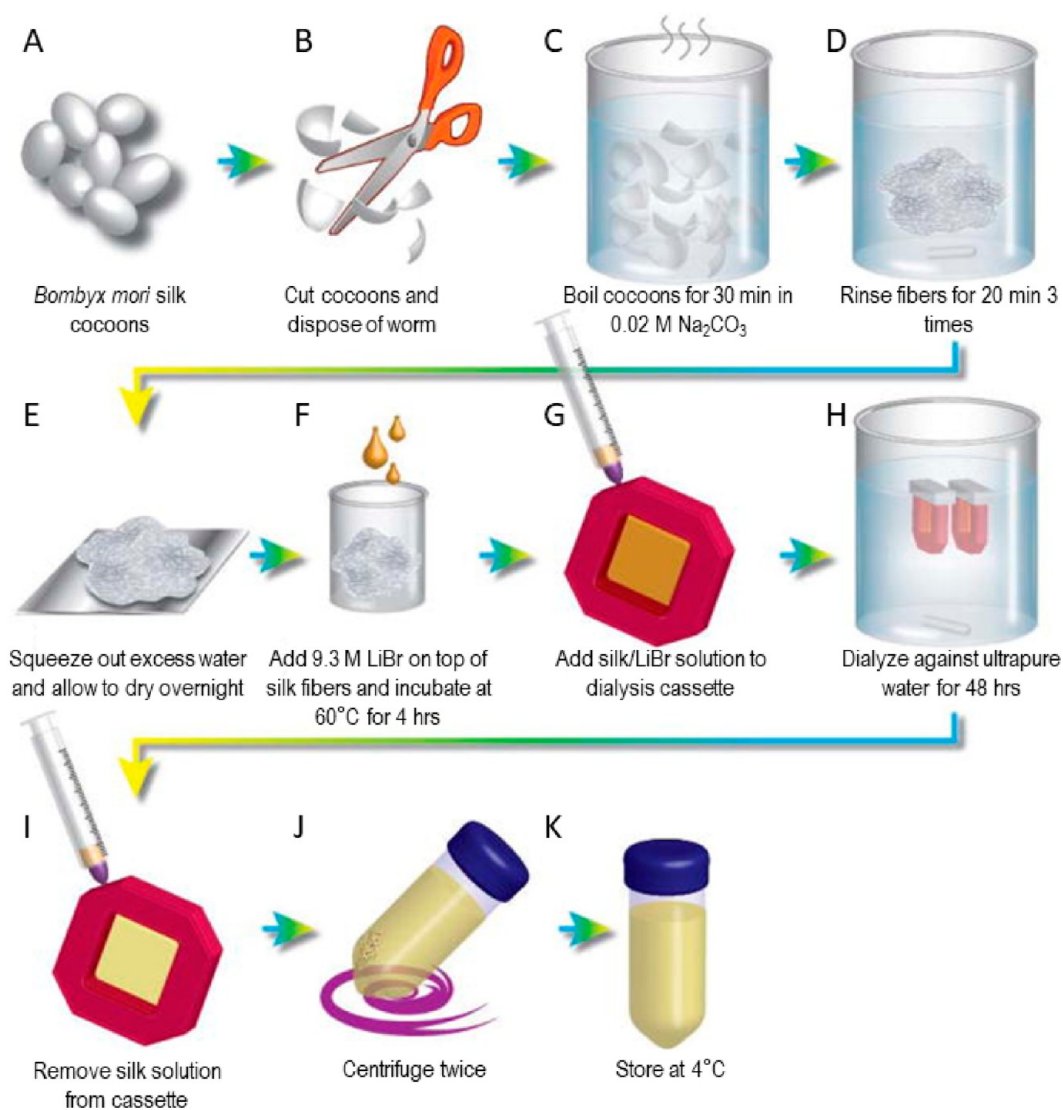


**Figure 4.** Procedure for extracting SF from *Bombyx mori* silk cocoons. (A) Whole *Bombyx mori* cocoons which are (B) cut up and the worm is removed. (C) Cocoons are boiled in a 0.02 M Na<sub>2</sub>CO<sub>3</sub> solution to dissolve sericin from native silk fibers, and (D) the fibers are rinsed with distilled water to remove any additional base before (E) being left to dry overnight within a fume hood. (F) The dried and liberated fibers are dissolved with 9.3 M LiBr at 60 °C for 4 h before (G) adding the solution to a dialysis cassette and (H) dialyzing against ultrapure water for 48 h. (I) The solution is removed from the dialysis cassette and (J) centrifuged twice to remove any impurities (i.e., parts of the silk worm that made it through this process). (K) The final solution is stored at 4 °C to prevent degradation. Adapted from Rockwood et al.<sup>40</sup> with permission from Macmillan Publishers Ltd., *Nat. Protocols*. Copyright 2011.

from their sericin “glue”, followed by dissolving into a 9.3 M solution of LiBr.<sup>34</sup> Purified silk is obtained by dialysis against water to remove the LiBr (Figure 4). Silk fibroin has been extensively processed into at least six different material classes: films, microspheres, tubes, sponges, gels, and fibers (Figure 3C).<sup>41</sup> Each of these different classes of materials possesses a unique structure and set of properties, and each has been tested as ECMs for cell culture. Films of SF have been well studied, with a long tradition as a medium of choice to promote cell growth, including neuronal growth, in culture.<sup>42</sup> Transforming films into three-dimensional scaffolds can be achieved by creating materials such as gels and sponges from silk fibroin that allow for a variety of cells to be grown into a tissue in three dimensions. A prime example of the use of 3-D silk scaffolds for neuroengineering is shown in work presented by Huang et al. using silk composite materials to grow and reconnect neural tissue in severed sciatic nerves in vivo.<sup>43</sup>

**Silk Materials as Artificial ECM 2-D Coatings.** Thin films and coatings of silk have been extensively studied as artificial ECMs for a variety of cells, including Chinese hamster ovary,<sup>44</sup> endothelial,<sup>45</sup> and cardiac cells;<sup>46</sup> however, within the context of this review, we will focus on studies that culture neurons, which are highly specialized cells that are among the most demanding to maintain in vitro. A widely used standard substrate for neuronal cell culture is a coating of polylysine, either the naturally occurring poly-L-lysine (PLL) or artificial mirror form poly-D-lysine (PDL). These are stereochemically distinct but otherwise chemically identical and possess strong positive charges along the polymer chain that are thought to promote neuronal adhesion and be permissive for the extension of axons and dendrites. Silk does possess some of these characteristics, having amino acids that can be independently pH-adjusted to create positive charges along the polymer backbone to modify cell attachment. Silk’s  $\beta$ -sheets allow for these polymers to remain water-insoluble yet

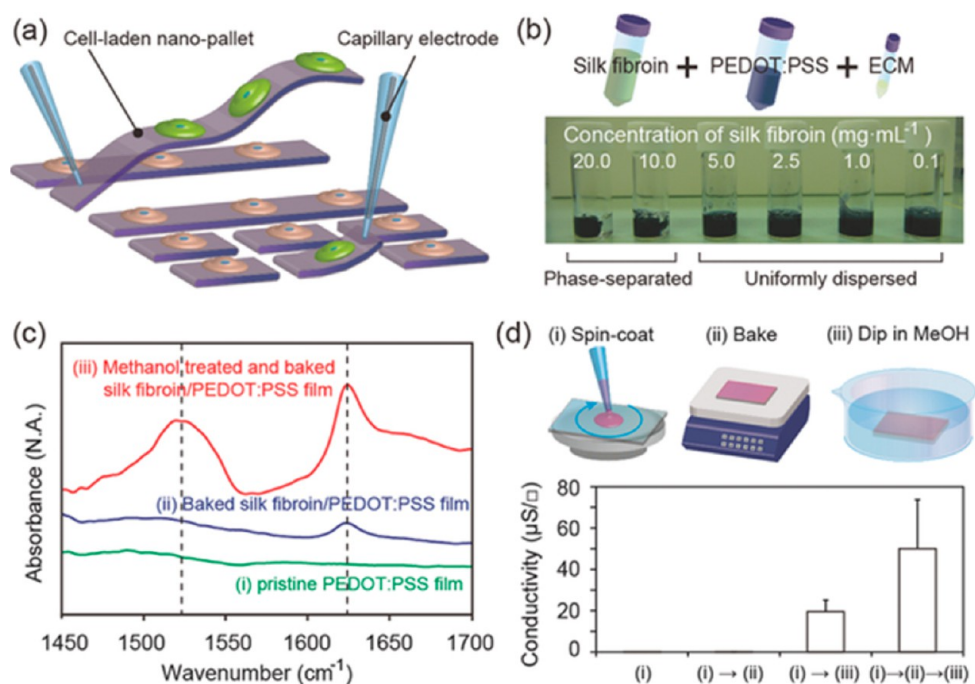


**Figure 5.** (a) Schematic representation of a device used to observe the electrical stimulation of cells with voltage-gated Ca<sup>2+</sup>-selective ion channels (Ca<sub>v</sub>2.1). When the channel is closed, no fluorescence is detected, but as the channels opens, a signal is emitted by the Ca<sup>2+</sup>-Fluo-4 dye complex (ex/em 494/506 nm). (b) Material composition of the mobile nanopallets and photographs of the resulting dispersions of the nanopallets in water. (c) FTIR spectra of the PEDOT:PSS film (green), baked SF/PEDOT:PSS film (blue), and methanol-treated and baked SF/PEDOT:PSS film (red). These FTIR spectra show the development of the β-sheet domain, characteristic of water-insoluble silk. (d) Evolution of electrical conductivity that is accompanied by (i) spin-coating, (ii) baking, and finally (iii) dipping in methanol. Reprinted from Teshima et al.<sup>52</sup> with permission from John Wiley and Sons, *Adv. Funct. Mater.* Copyright 2016.

swell with water to lower the elastic modulus.<sup>39</sup> A good examples of this was presented by Yang et al., who explored the use of *B. mori* silk films as a growth-promoting substrate for rat dorsal root ganglia (DRG) sensory neurons from the peripheral nervous system (PNS).<sup>47</sup> Using these silk fiber films, they demonstrated excellent biocompatibility for DRG neurons and promoted the survival of Schwann cells (SC), with minimal cytotoxic effects on cell function. A subsequent paper extended these findings using CNS hippocampal neurons, again demonstrating good biocompatibility and minimal cytotoxicity as indicated by normal morphology and good cell viability compared to the same properties of hippocampal neurons on PDL surfaces.<sup>48</sup> In both cases, the silk performed as well as or better than the typical substrate used to grow these cells.

Thin films have been extensively studied as a coating for cell culture dishes; however, coatings that incorporate SF or SF-modified polymers have opened new avenues to coat other biomedical devices such as neuronal probes and electrodes<sup>42,49</sup> and scaffolds for regenerative medicine.<sup>43,50,51</sup> SF has been used in conjunction with highly specialized neural probes as an inert, biocompatible, pliable, and tough structural component.<sup>49</sup> Teshima and co-workers microfabricated small electrode cell culture substrates, called nanopallets, composed of a highly cross-linked SF hydrogel matrix along with poly(3,4-ethylenedioxythiophene)/poly(styrenesulfonate) (PEDOT:PSS) conductive polymers.<sup>52</sup> In this case, the SF hydrogel coats the conductive PEDOT:PSS fabricated electrodes, enhancing the biocompatibility of the device while minimizing electrical resistance and remaining essentially optically transparent. This allowed the authors to electrically stimulate the cells while monitoring the activation of voltage-sensitive Ca<sup>2+</sup> channels with fluorescence

(Figure 5). In this example, the silk fibroin provides a soft and biocompatible coating for the hard and electronically conductive PEDOT:PSS nanoelectrodes.

**Patterned Silk Coatings for Substrates.** Patterning SF to direct neuronal growth has been explored<sup>53,54</sup> by adding topographical features (so-called 2.5-D surfaces) to flat 2-D films to allow for more precise control over neuronal process extension and positioning. These techniques have been extensively investigated for applications that aim to promote axon regeneration. The capacity to effectively pattern SF coatings has been applied to direct neurite growth and also as a means to roughen in order to present a more biologically permissive surface. Tan et al. have suggested that patterned SF coatings could form highly permissive and effective cochlear implants by promoting the formation of long-lasting associations with the spiral ganglion neurons that bridge peripheral and central auditory tissues.<sup>55</sup> Patterned cochlear implant coatings that increase surface roughness have promoted spiral ganglion attachment,<sup>55,56</sup> but directed neurite outgrowth has yet to be achieved by a similarly patterned surface, although several groups are actively pursuing this goal. Silk has emerged as the premiere material within this area, and several techniques have been employed to create patterned SF, including soft lithography<sup>57–59</sup> and physical processes.<sup>60</sup>

Hronik-Tupaj et al. demonstrated that SF patterning and daily uniaxial electrical stimulation cause neuronal processes to align along surface grooves (3.5 μm wide × 500 nm deep).<sup>60</sup> Alignment was found only on nanopatterned surfaces, and the aligned neurons demonstrated an explicit response in the form of functional linear networks. It is also possible to pattern a surface by including a chemical gradient within the silk material. For

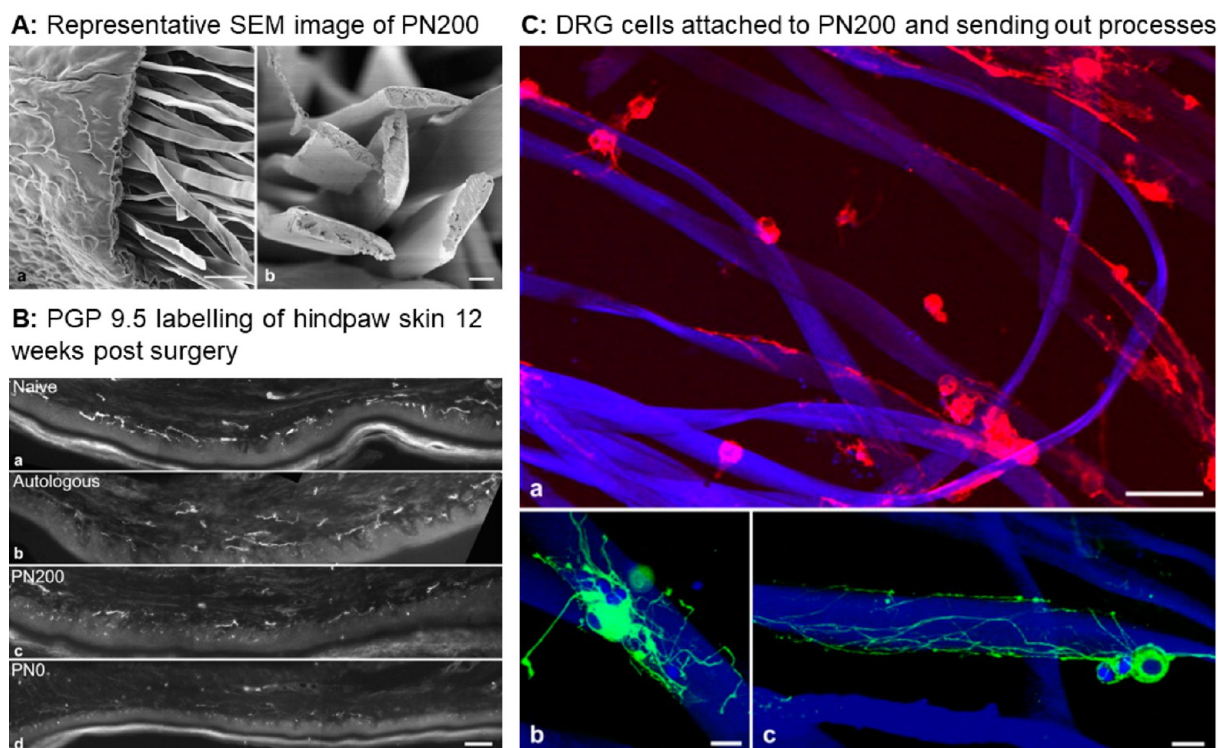


**Figure 6.** Composite figure demonstrating axon regeneration across 8 mm gaps in a rat sciatic nerve. (A, left) Representative scanning electron microscope image of a PN200 graft (consisting of 200 luminal silk fibers) displaying the outer sheath and (A, right) inner aligned luminal silk fibers. (B) Left hindpaw skin 12 weeks postsurgery labeled with PGP 9.5 to mark axons. The four conditions tested were (B, a) a naive animal group, (B, b) an autologous group, (B, c) PN200, and (B, d) PNO (a graft containing no luminal fibers). The autologous group (B, b) appears to have immunoreactivity that is similar to that of the naive group (B, a), while PN200 (B, c) demonstrated reduced PGP 9.5 immunoreactivity as compared to that of the autologous group. Few neurons were found on the PNO group (B, d). (C) Confocal images of adult DRG cells and their reaction with the silk graft. (C, a) Adult DRG cells attach to the degummed Spidrex fibers and put out processes, as labeled by phalloidin (red). (C, b) Neurofilament labeling shows the long extended neurites wrapping along the luminal fibers and (C, c) the Spidrex fibers. Adapted from Huang et al.<sup>43</sup> with permission from Elsevier, *Biomaterials*. Copyright 2012.

example, the creation of a NaCl gradient generated a gradient of porosity within the resulting silk film. Neurons specifically grew best where the porosity was highest, showing a general trend toward higher salt content (larger numbers of pores).<sup>61</sup> Such patterned surfaces could direct neuronal process extension, with potential future materials being employed in neuro-regenerative medicine. A prime example of these neuronal guidance materials involves using aligned SF fibers that can act as physical guidance for growing neurites. Topographic patterns of the correct size regime, typically on the order of 100  $\mu\text{m}$ ,<sup>62</sup> have been extensively studied for their neurite outgrowth promotion and synaptogenetic properties, yet few studies have combined topographically functionalized surface patterns with a chemoattractant with the goal of directing axon or dendrite guidance. With the goal of promoting regenerative growth in the CNS, Madduri and co-workers describe SF nanofibers functionalized with the glial cell-line-derived neurotrophic factor (GDNF) and nerve growth factor (NGF).<sup>63</sup> A series of experiments used aligned and nonaligned functionalized SF to examine neurite outgrowth from explants containing embryonic chick spinal cord motor neurons and embryonic PNS DRG neurons. Directional outgrowth was observed only along the aligned SF fibers as compared to the randomly arranged fibers which were no different than the control. This approach used SF fibers patterned with NGF and GDNF to demonstrate the benefit of employing both a chemoattractant and physical cues to guide neurite outgrowth.

**Silk Scaffolds in 3-D.** Transitioning from two-dimensional films to three-dimensional neural networks, scaffolds are being

employed to investigate cellular mechanisms using culture conditions that aim to more closely mimic the native environment *in vivo*. This is especially important for neurons since neural networks are inherently three-dimensional rather than the thin, relatively two-dimensional space presented by a typical cell culture dish surface. Three-dimensional scaffolds may incorporate physical channels, grooves, or supports. An example of such haptotactic physical guidance is the support of neuronal growth by uniaxial channels ( $\sim 42\text{--}142\ \mu\text{m}$ ) within a silk sponge.<sup>32</sup> These structures were created by generating cylindrical ice crystals via a directional temperature field freezing technique. The material then functioned as a directional sponge, confining neuronal growth and directing neurite process extension along one axis. Using embryonic mouse CNS hippocampal neurons, axons projected along the sponge—scaffold holes. Such scaffolds were further refined by aiming to generate gels that mimic the modulus of human tissues, creating SF hydrogels that range from 4 to 33 kPa, while maintaining structural integrity.<sup>64</sup> In this study, explants of embryonic chick PNS DRGs were embedded in SF hydrogels, and axon growth was assessed. Modulus matching was found to promote outgrowth from the explants, with the best occurring on 2 and 4% silk hydrogels.

The potential of SF scaffolds to function as silk conduits to promote peripheral nerve regeneration in adult rats has recently been examined by several groups, and silk is among one of the most promising materials for neuroregenerative medicine currently being explored.<sup>65,66</sup> By employing SF in conjunction with a spider silk mimic (Spidrex), Huang and co-workers were



able to achieve partial axonal regeneration across up to 13-mm-long gaps in rat sciatic nerve.<sup>43</sup> In this study, regeneration was enhanced over the 12 week period monitored. Four weeks after injury, Huang's best nerve-repairing conduits regenerated ~62% (mid conduit) and ~59% (distal to injury) of the previous neuronal density as compared to autologous nerve graft controls. Compared to the controls, the silk conduits limited the inflammatory macrophage response and supported colonization by Schwann cells, the myelinating glial cells that electrically insulate axons in the PNS (Figure 6). After 12 weeks, regenerated axons were myelinated to an extent similar to that of uninjured controls (81%). Such findings suggest that SF scaffolds have a substantial potential to promote recovery following nerve damage.

An example of the application of silk scaffolds to promote nerve regeneration by Gu and colleagues provides an innovative twist. By combining cell-derived ECM components with silk and chitosan, to further tailor the structure and modulus of the graft, they report regeneration across up to ~10 mm gaps in the adult rat peripheral nerve, similar to those described in Huang's paper.<sup>43</sup> While the two papers demonstrate similar methods of achieving comparable results, Gu's approach involves impregnating the graft with reconstituted ECM from Schwann cells or from acellular sources (e.g., NeuraGen, NeuroMatrix, Neuroflex, NeuraWrap, and NeuroMend, all proprietary and complex blends of polymers from cellular sources).<sup>51</sup> The chitosan and SF surfaces were cultured with SCs to create ECM derived exclusively from the cellular source but were subsequently decellularized to create an ECM-functionalized chitosan–SF graft (Figure 7).<sup>51</sup> This approach provides two potential benefits: (1) it creates a highly tailored nerve graft that can be derived from green, renewable feedstocks and (2) histopathological and blood parameters indicated that this approach maximizes safety and limits the macrophage response, which could lead to a rejection of the graft. Electrophysiological measurements confirm a sizable recovery over 12 weeks, albeit not to uninjured levels. Interestingly, using electrophysiological measurements as a matrix for recovery, naked scaffolds were significantly less effective than acellular and SC-derived ECM; however, no significant difference was found between Schwann cells and acellular derived ECM.<sup>51</sup> The approach of using silk as a scaffold for cellular-derived ECM is innovative and highlights silk's biocompatibility since the naked silk–chitosan scaffolds do not evoke a significant immune response.

**SF-Based Composite Materials.** While silk fibroin alone has proven to be a successful scaffold to support three-dimensional neuronal networks, multicomponent composite materials allow further tailoring of the surface conditions to promote neuronal growth and survival. Ren et al. employed a hyaluronic acid (HA) SF composite scaffold that exhibits particularly high porosity (~90%).<sup>67</sup> These highly porous scaffolds have a tunable HA content, which influences neuronal adhesion and attachment. Pore sizes ranged from 123 to 253  $\mu\text{m}$ , allowing for large water content absorption, with the material swelling to up to 10% by volume. HA-generated scaffolds that were more hydrophilic compared to similar SF-only electrospun materials were added. SFs have also been incorporated into a variety of polymers such as chitosan and poly(L-lactic acid-co- $\epsilon$ -caprolactone) to modify their properties.<sup>68–70</sup> Some of these modified scaffolds have been tested for their capacity to promote axon regeneration in rat sciatic nerves following injury. One strategy employed chitosan–SF composite materials as a delivery vehicle for adipose-derived stem cells which promoted the repair

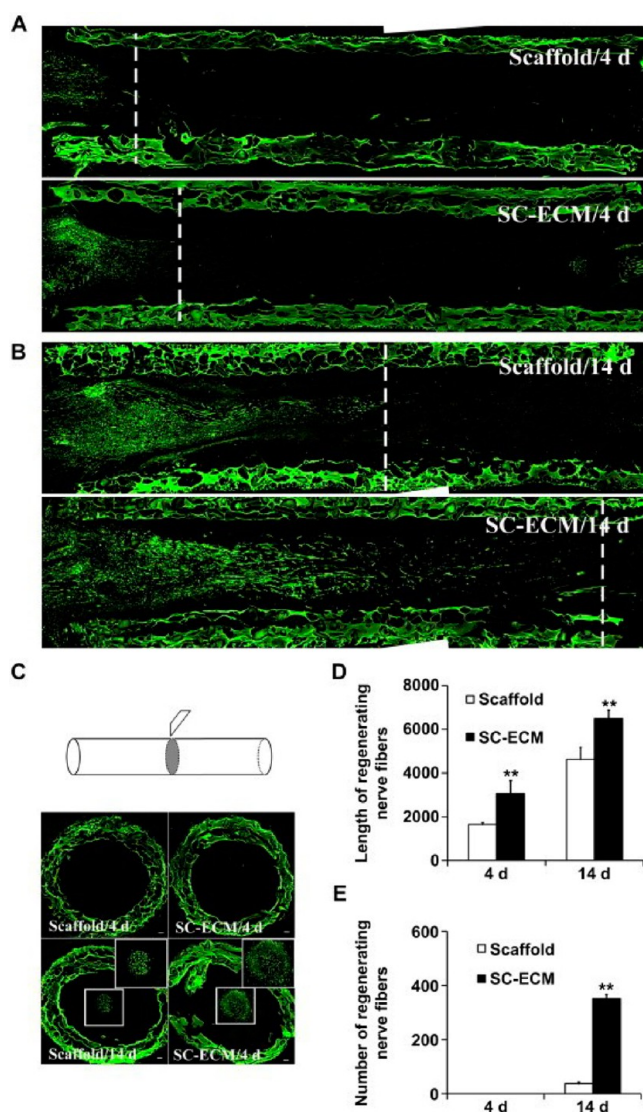


**Figure 7.** Neurofilament immunohistochemical staining of rat sciatic nerves within the bridged 10 mm gap. The dotted line represents the front of axon growth within the denoted period. (A) Longitudinal section of a plain chitosan/silk graph (top) and the SC-ECM derived graph (bottom) after 4 days. (B) Sections of the plain chitosan/silk graph (top) and SC-ECM-derived graph (bottom) after 14 days. (C) Transverse sections of the nerve graph showing the thickening edge with the SC-ECM compared to just the scaffold after 14 days. (D) Histogram of the length of regenerating axons vs the surgery date (4 and 14 days) and (E) number of regenerating nerve fibers. (\*\* $p < 0.01$ ). Reprinted from Gu et al.<sup>51</sup> with permission from Elsevier, *Biomaterials*. Copyright 2014.

of gaps in sciatic nerves across a 10 mm distance.<sup>71</sup> Poly(L-lactic acid-co- $\epsilon$ -caprolactone)–SF blends were employed in electrospun peripheral nerve grafts, demonstrating enhanced regeneration and recovery of nerve function by 8 weeks following injury.<sup>72</sup> Wang et al. attributed the enhanced regeneration to the alignment of the nanofibers in the SF–synthetic polymer blends as well as using a combination of a soft material, such as SF, along with cellphilic poly(L-lactic acid-co- $\epsilon$ -caprolactone), which has recently been shown to dramatically increase the adhesion of neural cells.<sup>73</sup> A final example of the application of SF composite materials supports the generation of engineered layered brain tissue.<sup>74</sup> This achievement capitalizes on a number of the best

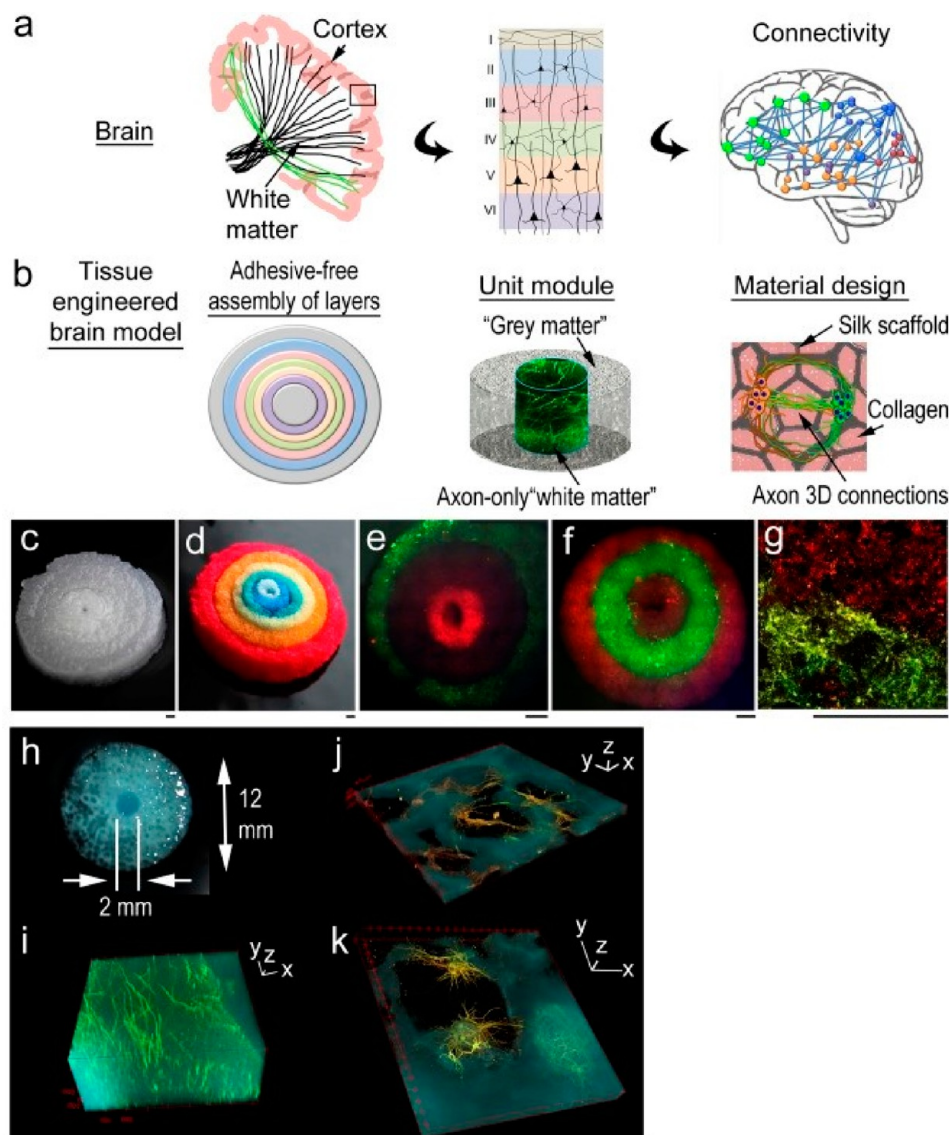


**Figure 8.** Using SF and collagen gels to create a modulus-matched toroid, generating cortical-like tissue organization in vitro. (a) Illustration of the organization of white matter and six layers of neocortex. (b) Design strategy that aimed to mimic these natural structures within a new material. (Left) Adhesive-free assembly of concentric layers (similar to the layers within the neocortex) and (middle) the unit module consisting of neuron-rich gray matter regions along with axon-only white matter regions. (right) Demonstration of the material design showing the scaffold and collagen gel composite material supporting connections in 3-D. (c) Photograph showing the three-dimensional silk scaffold and (d) a dyed version of the same layered toroid to aid in visualization. (e) Photograph of the toroid seeded with different primary rat cortical neurons (live stained with DiI in red and DiO in green) and (f) a photograph after cells were grown. (g) Representative photograph of the interface between each of the populations (scale bar 1 mm) (h) Photograph of the scaffold showing the dimensions along with (i) confocal z-stack multichannel images of 3-D brainlike tissues labeled with axonal marker  $\beta$ 3-tubulin in green and dendritic marker microtubule-associated protein-2 in red. This confocal stack is from the center axon-only region, while (j) and (k) are from porous regions within the scaffold. Adapted from Tang-Schomer et al.<sup>74</sup> with permission from the National Academy of Sciences, *Proc. Natl. Acad. Sci. U.S.A.* Copyright 2014.

attributes of SF, in particular, its soft modulus in conjunction with its high water content, while the collagen was introduced to structure a layered toroidal doughnut-like architecture that was used to model different parts of the brain by varying the modulus of each layer (Figure 8).

**Polyelectrolyte Multilayers as Tunable Coatings.** The previous section outlined how a naturally derived self-assembled polymer such as silk can be modified and employed as a replacement for neural ECM. It is clear that cells respond to the stiffness of their substrate, and thus altered mechanical properties, such as Young's modulus, can directly impact cell survival and development.<sup>75</sup> A key technique to controlling the

modulus and other properties of an engineered surface is to assemble polymers using a layer-by-layer approach. LbL assemblies were first introduced by Decher et al. in the early 1990s as a substitute for chemisorption via the classical Langmuir–Blodgett technique. LbL assembly relies on electrostatic interactions between two oppositely charged polyelectrolytes as the main driving force for a facile bottom-up method of preparing ultrathin films that removes the need for covalent bond formation and a dependence on substrate size and morphology.<sup>76</sup> Other interactions such as hydrogen bonding or charge-transfer interactions can also drive the assembly process, highlighting the versatility of the LbL approach. Since

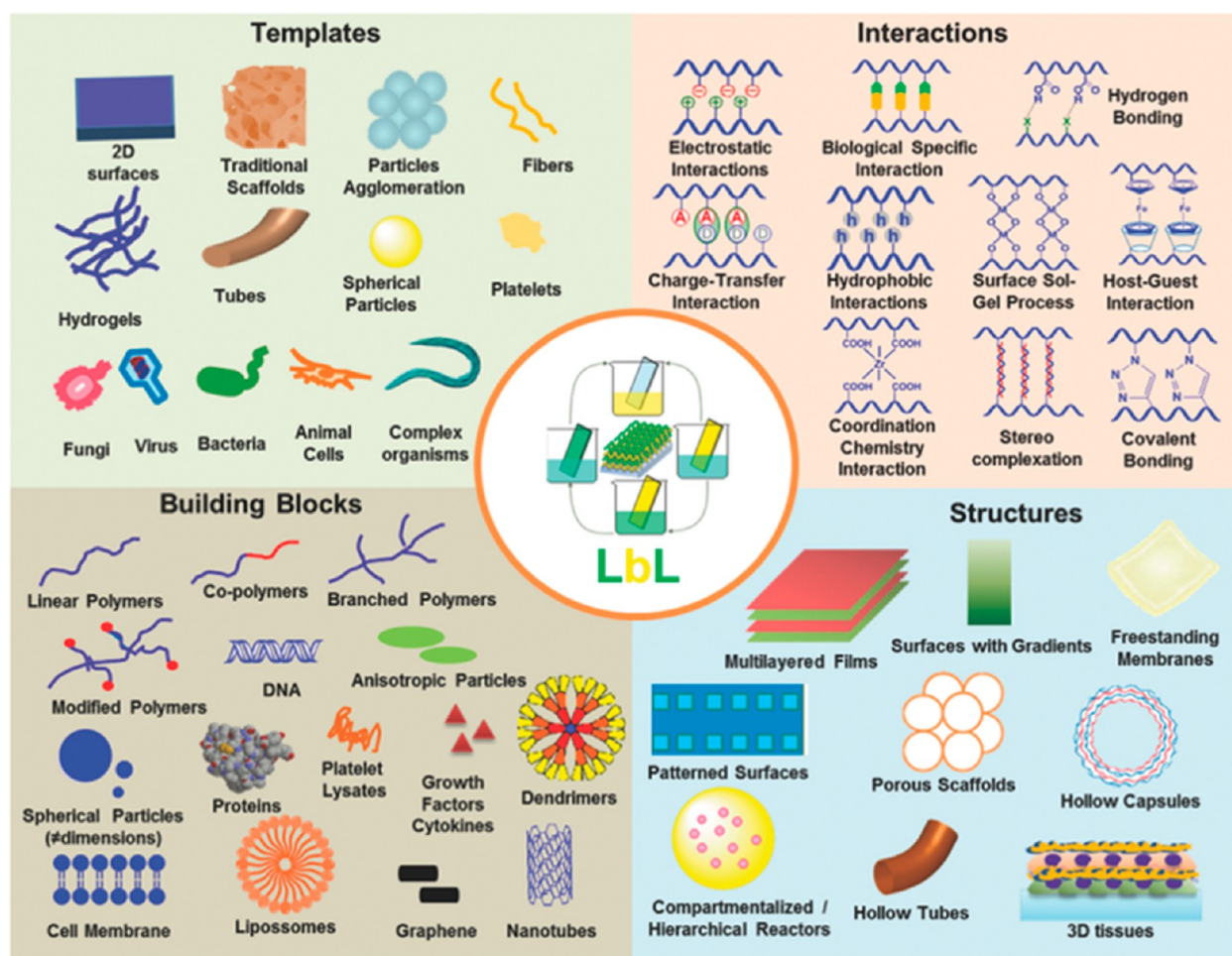


**Figure 9.** Summary of the scope of LbL assembly techniques showing possible interactions between polymer layers, the different building blocks available, the structures created, and templates. Reprinted from Silva et al.<sup>83</sup> with permission from John Wiley and Sons, *Small*. Copyright 2016.

the introduction of this technique, LbL assemblies have been used as an easy and inexpensive method to functionalize a wide variety of surfaces. The overall technique relies on dipping a surface into an aqueous solution of charged polymer, rinsing, and dipping into a solution that contains the complementary oppositely charged polymer. The charge-overcompensating alternating process then repeated until the desired number of layers have been deposited (Figure 9, inset). The properties of these surfaces can be easily tuned by modifying the nature of the interaction between the two polymer layers, the nature of the building blocks of the films, such as using synthetic polyelectrolytes,<sup>77</sup> polypeptides,<sup>78,79</sup> or polysaccharides,<sup>80</sup> and by tuning the preparation conditions.<sup>81,82</sup> Since its first description, structures more complex than simple films have been prepared using LbL techniques, and these structures can be modified to be responsive to stimuli.<sup>83</sup> A summary of the scope of this technique is illustrated in Figure 9. Because the technique offers minute control over surface properties, a substantial number of the research efforts toward these ultrathin films has focused on their potential application as biomaterials.<sup>84</sup> Previous studies took advantage of the mechanical properties of LbL thin films, such as their dynamic stiffness,<sup>85</sup> or mechanical compliance,<sup>86</sup> to modulate cell adhesion. Published reviews offer comprehensive descriptions of LbL surfaces, focusing on their general physical, biochemical, and mechanical properties.<sup>87,88</sup> A comprehensive review of biopolymer-based LbL

surfaces has been published,<sup>83</sup> and Silva et al. have addressed their use as engineered extracellular matrixes.<sup>83</sup>

LbL-derived films have been exploited as cell culture surfaces and coatings for a range of cell types;<sup>83</sup> however, a complete exploration as potential growth surfaces for neurons is lacking. LbL coatings offer an attractive interface between biological and artificial materials due to their versatility, and LbL deposition techniques have been used to create polymer assemblies in areas such as macromolecular encapsulation<sup>89,90</sup> and biocompatible coatings for artificial implant materials.<sup>90,91</sup> Because of their complementary charges that can be controlled via the pH of the dipping baths, poly(acrylic acid) (PAA) and poly(allylamine hydrochloride) (PAH), which are simple polymers of acrylic acid or allylamine, respectively, are two of the most commonly used synthetic PEs in the fabrication of PEMs. Research from our groups on PAA/PAH PEMs has shown that the fabrication conditions play a key role in altering the PEM surface properties and modulus.<sup>92,93</sup> By varying the number of layers, the PEs used, or the deposition pH, an almost infinite number of physically unique PEMs can be created. Previous work in this field has focused mainly on the adhesion, viability, differentiation, and proliferation of neural cells on LbL thin films for use as ECMs.<sup>87,94</sup> Here, we highlight the more recent reports and focus on the dependence of performance on the physical properties of the materials and their suitability for potential use as surfaces to study the function of neural cells.

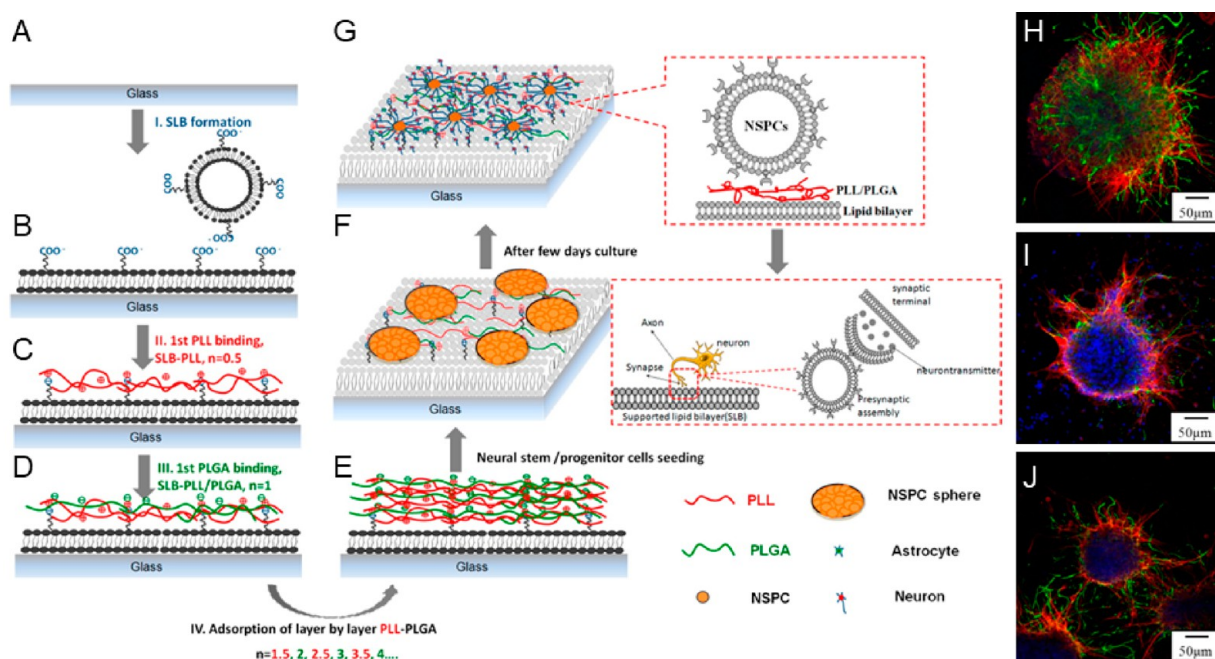


**Figure 10.** (A–G) Schematic representation of the fabrication processes of the multilayer coatings: (A) a fresh glass surface hosts a (B) supported lipid bilayer lysed onto the surface, exposing the functionalized negatively charged ( $-\text{COO}^-$ ) groups and allows for (C) PLL (positively charged polymer) to layer onto the surface followed by (D) PLGA (negatively charged polymer). (E) The PLL/PLGA multilayer is built up to the desired number of layers before (F) NSPC spheres were cultured onto the plate. (G) A schematic view of the culture is seen with the resultant images shown on the left (H–J). Fluorescent images show the cellular phenotypes that differentiated depending on the LbL surface conditions. Anti-MAP-2 (red, neurons) and anti-GFAP (green, astrocytes) label the differentiated cells. (H) A thinner surface results in more astrocytes ( $n = 3.5$ ) and (I) a supported LbL PEM of 7.5 layers and finally (J) a PEM with 8 bilayers. Adapted from Lee et al.<sup>100</sup> with permission from the American Chemical Society, *ACS Appl. Mater. Interfaces*. Copyright 2014.

### Layer-by-Layer Coatings Incorporating Natural Growth Factors and Polymers.

LbL assemblies can play host to a variety of different polymer combinations and properties dictated by assembly conditions so that if they are carefully chosen then these artificial polymers can take on the appearance and feel of real ECMs. One can mimic an ECM by selecting soft and biologically permissive polymers (such as PLL and HA) and incorporating components of the natural ECM as a method to biocamouflage LbL assemblies on surfaces. In principal, these biocamouflaged surfaces represent a more natural, albeit engineered, environment that can be tailored and optimized for neuronal survival and growth. Zhou and colleagues highlight the capacity of LbL assemblies to biofunctionalize surfaces for the survival and growth of neural progenitor cells (NPC).<sup>95</sup> Previous work has focused on the use of hard yet supportive monolayers of bioresponsive polymers (such as PDL, PLL, HA, etc.), but Zhou et al. focused on using cellular-derived ECM components in combination with an LbL approach to support the growth of NPCs. Poly- $\epsilon$ -caprolactone, a material previously used both in vitro and in vivo for neural tissue engineering, was functionalized with an LbL thin film of PLL and heparin sulfate or brain-derived neurotrophic factor (BDNF) with the aim of creating a coating that promotes regeneration while minimizing spinal cord injury inhibitory environments.<sup>95</sup> The effectiveness of this surface was assayed by quantifying the length of extending neurites and biochemical correlates of growth.

PLL was demonstrated to play a crucial role as a positively charged polyelectrolyte within an LbL assembly that supports the electrostatic binding of growth factors while itself being a biopermissive polymer.<sup>83,95</sup> Because of highly tailorable surface

properties (such as charge, modulus, and porosity), LbL thin films represent a promising platform for incorporating growth factors into a surface, due in part to adhesive ionic interactions on the surface and within the structure of these films. Electrostatically bound small molecules, growth factors, and drugs on highly charged LbL films have been investigated,<sup>96</sup> yet the incorporation of ionically bound ECM components remains one area that has been sparsely developed for any cell type. Functionalizing an LbL thin film with biologically active proteins has substantial potential to optimize neuronal adhesion, survival, and growth.<sup>97,98</sup> As a demonstration of this, Vodouhê and co-workers created a biofunctionalized LbL assembly composed of poly(ethylene-imine), PLL, or PAH as polycations and poly(sodium-4-styrenesulfonate) (PSS) or poly(L-glutamic acid) as polyanions along with BDNF and Semaphorin 3A as growth and tropic factors. Their approach embedded the proteins during the assembly process, with zwitterionic interactions providing stability.<sup>99</sup> This proved to be a facile technique for creating bioactive surfaces that present the growth factor and chemotropic factor, in conjunction with permissive polymers, to determine their influence on the growth of embryonic mouse spinal motoneurons.<sup>99</sup> Characterizing the morphology of cultured spinal motoneurons, they found that BDNF-containing surfaces had enhanced survival above the control (an 84% increased survival rate). The stability of BDNF in the substrate was found to be critical, as leaching of the incorporated BDNF significantly lowered the viability over time, and LbL assemblies containing PSS/BDNF exhibited minimal leaching and thus performed best, as compared to PSS and PLL surfaces.<sup>99</sup>

Lee et al. developed a method to culture, differentiate, and promote neurite outgrowth using amino acid-containing

polymers such as PLL and poly-L-glutamic acid (PLGA). Assemblies of PLL and PLGA were layered onto supported lipid bilayers and used to induce neural stem/progenitor cells to migrate from cultured neurospheres and differentiate into neurons without the need for added serum or growth factors.<sup>100</sup> The neurite outgrowth length and the percentage of differentiated neurons were quantified relative to the number of layers of PLL/PLGA. The induction of differentiation occurred on films of up to eight layers thick. The charge of the last layer was found to influence neurite outgrowth and synaptogenesis, as positively terminated surfaces (PLL) out-performed negatively terminated (PLGA) surfaces as measured by immunocytochemically labeling presynaptic synapsin I and dendritic MAP-2 (Figure 10). Lee, Vodouh , and Zhou's work highlights the benefits of combining naturally derived ECM materials with synthetic polymers in LbL-assembled materials and illustrates the flexibility, ease of use, and power underlying the capacity of this technique to create highly functional surfaces/coatings to support neurons in cell culture.

#### Tailored LbL Assemblies to Control Surface Charge.

Multilayered surfaces can be tailored and specialized based on deposition parameters and even polymer choice, providing surfaces that can influence neural cell migration, adhesion, and differentiation. Cellular differentiation is an important aspect to study as surfaces have been found to influence the differentiation of neural stem/progenitor cells to functional neurons based on the physical properties of a LbL surface, such as charge,<sup>101</sup> modulus,<sup>14</sup> and chemical functionality.<sup>102</sup> Since all of these physical properties can be highly tuned based on polymer choice or deposition parameters, LbL-created assemblies remain the platform of choice for the exploration of these biological phenomena. Ren et al. studied the effect of changing pendant functional groups on polymeric assemblies for the differentiation of NSCs to functional neurons.<sup>103</sup> The studied pendant side-chain functionalities included hydroxyl ( $-\text{OH}$ ), sulfonic ( $-\text{SO}_3\text{H}$ ), amino ( $-\text{NH}_2$ ), carboxyl ( $-\text{COOH}$ ), mercapto ( $-\text{SH}$ ), and methyl ( $-\text{CH}_3$ ) groups and demonstrated a range of contact angles revealed by measurements of neural stem cell morphology.<sup>103</sup> Sulfonic acid-functionalized surfaces differentiated neural stem cells into oligodendrocytes, while carboxyl-, amino-, mercapto-, and methyl-decorated LbL assemblies differentiated neural stem cells into a mixture of astrocytes and oligodendrocytes. Ren and co-workers hypothesized that the hydrophilicity of the surface had a dramatic effect on neural stem cell differentiation as evident from dramatic differences between the transformed cell types seen as a function of their contact angle (between methyl and sulfonic acid groups).<sup>103</sup>

While pendant side-chain functionalities appear to have a significant influence on the differentiation of neural stem cells to neural cell types, other surface properties such as the charge and modulus may also influence this process. Lee and co-workers investigated a PLL/HA system for the differentiation of neural stem/progenitor cells into different lineages (neurons, astrocytes, and oligodendrocytes) by studying the effect of surface charge and the number of layers in these LbL-assembled systems.<sup>4</sup> Neural stem/progenitor cells were induced on films as thin as monolayers; however, the percentage of differentiated neurons increased with increasing coating thickness up to a maximum of four bilayers, after which no discernible difference was determined.<sup>4</sup> Single lineage induction was never achieved, and only heterogeneous populations of differentiated cells were found. Cellular phenotypes were determined by immunostaining with MAP-2 (neuron) and GFAP (astrocyte), and the film

thickness, and as a result the elastic modulus, was found to influence the ratio of neurons to astrocytes somewhat, with astrocyte counts decreasing with increasing film thickness. Charge was also studied and found, perhaps surprisingly, to have little influence on the ability of neural stem/progenitor cells to be induced, in contrast to findings from Ren and co-workers. While charge now appears to exert little effect over the differentiation of neural stem/progenitor cells to neurons, it does influence the length of processes, as evident by neurite outgrowth assays on negatively and positively terminated surfaces. The longest process extensions were found to occur on positively terminated surfaces, providing a demonstration of the explicit control over cellular response as a function of the physical properties of a surface.<sup>4</sup>

**Tuning the Stiffness of LbL Coatings.** The physical and surface properties of LbL-assembled materials influence cellular function.<sup>14,23,31</sup> While charge and chemical functionality have been extensively studied,<sup>4,7,5,103</sup> one might aim to study the elastic modulus of the supporting material independently of the surface properties. Importantly, this bulk property of an LbL film can be tuned on the basis of layer thickness, water content, and polymer selection.<sup>104</sup> As an example to illustrate the influence of modulus on neuronal differentiation, Leipzig et al. created a methacrylamide- and chitosan-based biomaterial, with a tunable modulus (1–30 kPa), to study the influence of the modulus on the differentiation of neural stem/precursor cells.<sup>14,105</sup> They found that stiffer polymeric surfaces ( $>7$  KPa) resulted in the differentiation of neural stem/precursor cells to oligodendrocytes, whereas softer surfaces promoted the generation of astrocytes ( $<3.5$  kPa).<sup>14</sup> LbL-assembled films and coatings present a key opportunity to study the modulus of supportive coatings independent of surface properties (charge and chemical functionality) yet with a distinctly reproducible elastic modulus.<sup>106</sup> However, because of the enormous parameter space involved in the preparation and fine tuning of LbL thin films, we lack a clear structure–activity relationship between the modulus and the viability of LbL film candidates, primarily due to the absence of specialized tools required to efficiently study each parameter.

To address this, Sailer and Barrett developed a combinatorial method to create gradient surfaces, with variable modulus and thickness, to facilitate studying large parameter spaces on a single film for high-throughput screening.<sup>23,25</sup> The method could also prepare 2-D gradient films, representing a parameter space equivalent to many thousands of uniform films, that allowed for high-throughput combinatorial screening of film-layering parameters and the identification of conditions that enhance cell viability. To achieve this, thin films of PAH and PAA were prepared slowly and vertically, filling from the bottom up and varying the pH and salt concentrations of the polyelectrolyte solutions during their deposition. By adding reagents (acids, bases, and salts) with a syringe pump, this effectively changed the deposition conditions on the fly during film fabrication from bottom to top.<sup>23,25</sup> By rotating the film by  $90^\circ$  after each layer deposition, a full 2-D gradient surface could also be achieved. The cell viability was assayed using a HEK293 cell line, identifying the optimal pH range that created regions within the gradient film exhibiting the best survival. The apex of cell viability was found within a small range of deposition pH (pH 7–8 for PAH and pH 5–6 for PAA), demonstrating the power of effectively screening the equivalent of over 10 000 single films on one gradient surface. This work was extended to identify surfaces of optimal viability for embryonic rat spinal commissural

neurons, correlating the surface energy (wettability), matrix stiffness, and surface charge with cell survival and growth (Figure 11). For both HEK293 and commissural neurons, optimal

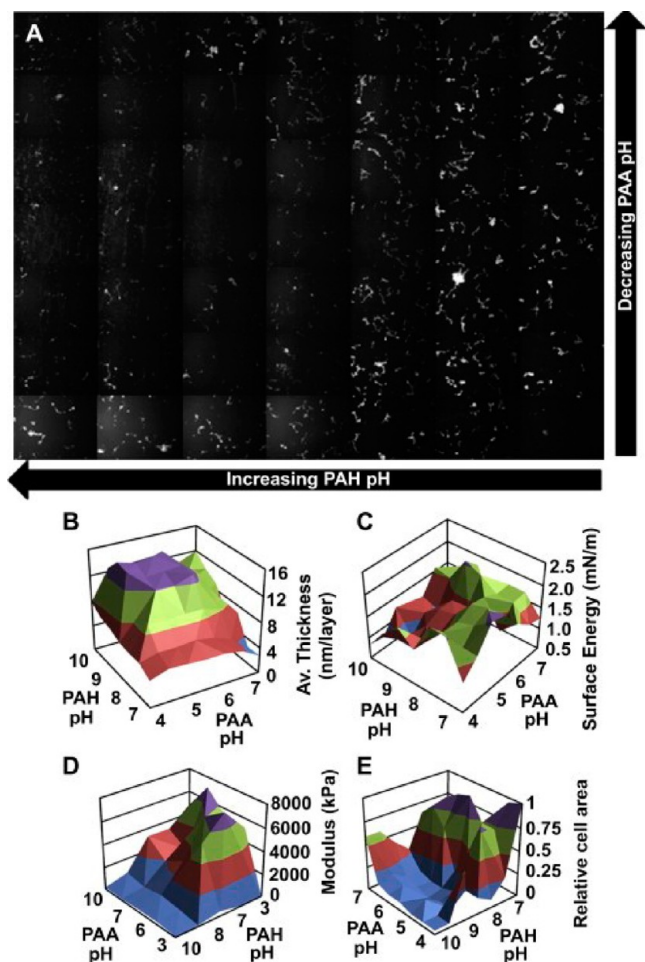


**Figure 11.** (A) Compilation of embryonic rat spinal commissural neuron morphologies at various points within the gradient surface. Microscope images shown in relation to 2-D properties of films depending on the pH of assembly of the polyelectrolytes. Plots of (B) average thickness, (C) surface energy (mN/m), (D) modulus (kPa), and (E) relative cell coverage vs PAA and PAH deposition pH. Reprinted from Sailer et al.<sup>23</sup> with permission from Elsevier, *Biomaterials*. Copyright 2012.

growth was detected at an intermediate modulus of between 500 and 800 kPa, and no cells survived in regions of the film that had a modulus below 500 kPa, consistent with a minimal level of mechanical support being required for attachment and growth.<sup>23,25</sup> This study supports the conclusion that survival and growth are highly influenced by the modulus, which is an important step toward attaining an in-depth understanding of cell–surface interactions.

**Advanced Applications in Biomedical Devices.** This discussion of LbL-fabricated materials has focused primarily on the physical aspects of coatings and their subsequent effects on the viability of neural cells in culture. An additional attractive, key feature of LbL assemblies is their flexibility. LbL assemblies have been demonstrated to coat a variety of substrates; consequently, applications toward biomedical devices have been explored due to the adaptability of LbL in creating coatings with enhanced biocompatibility on complex geometries, such as neural implants

and electrodes.<sup>101,107,108</sup> Applications have also included the direct patterning of substrates to influence and guide neural cell growth, adhesion, and viability. Kidambi et al. addressed the impact of astrocytic oxidative stress on neurons by creating patterned cocultures on LbL-assembled structures.<sup>109</sup> This patterning occurred without the use of expensive proteins or ligands and was created by direct microcontact printing of sulfonated poly(styrene) on poly(diallyldimethylammonium chloride)(PDAC)/sulfonated polystyrene surfaces. The placement of each member of the coculture (astrocyte and neuron) was achieved by their binding preference for either a negatively charged or positively charged area within the patterned film. Primary neurons preferentially attached to the negatively charged PSS layers, while the astrocytes attached to either layer with no preference (Figure 12).<sup>109</sup> The patterned surface was

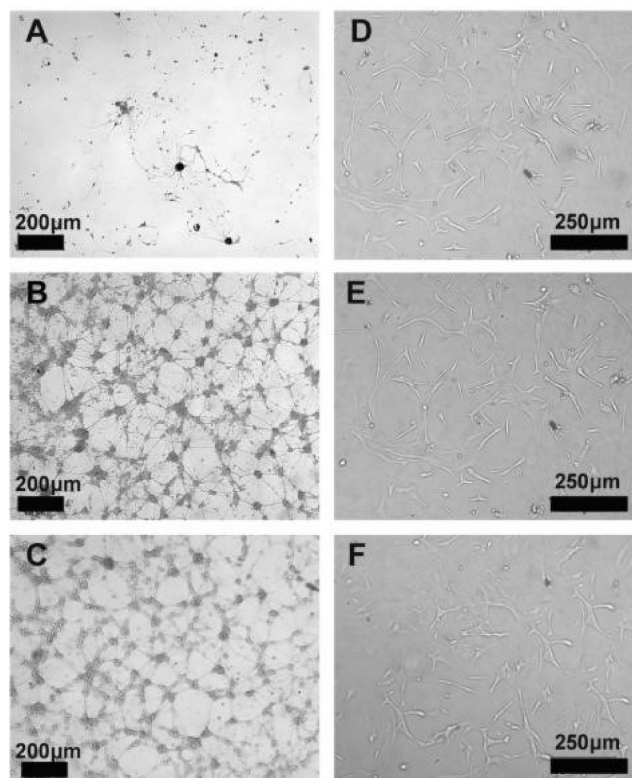


**Figure 12.** Phase-contrast images of primary neurons and astrocytes after 7 and 3 days, respectively, illustrating their morphology and growth patterns determined by the LbL substrate. Primary neurons were plated on (A) 10.5 layers of PDAC/SPS showing PDAC as the topmost layer, (B) 10 layers of PDAC/SPS showing SPS as the topmost layer, and (C) PLL as a control. Astrocytes were plated on (D) 10.5 layers of PDAC/SPS showing PDAC as the topmost layer, (E) 10 layers of PDAC/SPS showing SPS as the topmost layer, and (F) PLL as a control surface. Reprinted from Kidambi et al.<sup>109</sup> with permission from John Wiley and Sons, *Adv. Funct. Mater.* Copyright 2008.

used to study the neuronal response to high levels of reactive oxygen species that are associated with oxidative stress and contribute to neural pathogenesis and neurodegenerative diseases.<sup>109</sup> Using microcontact-printed LbL-assembled materials to precisely place neural cells in culture demonstrates both the utility and flexibility of this deposition technique.

Control over the resulting physical properties of a film can be achieved during the process of deposition, effectively locking in any physical property, such as the modulus. This limits the

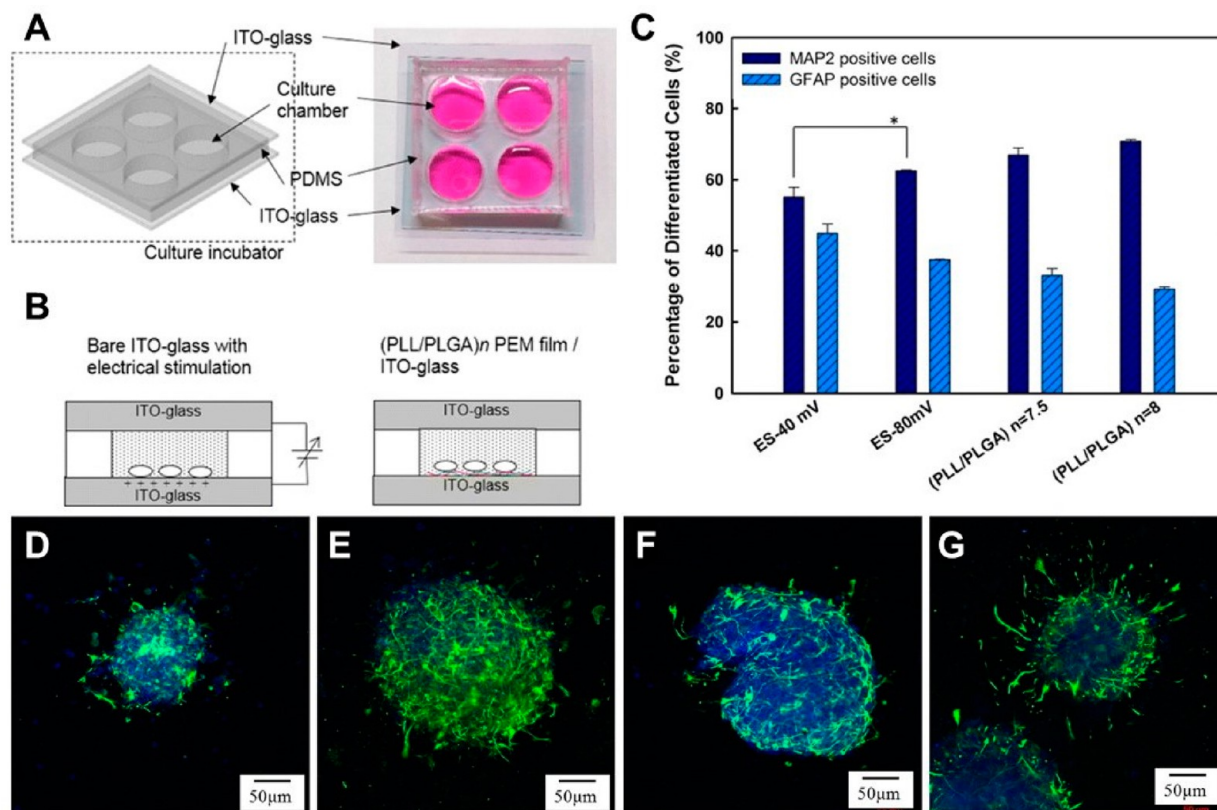


**Figure 13.** (A, left) Schematic drawing of the fabricated device showing the ITO glass and the PDMS chamber along with (A, right) a photograph of the resulting fabricated device. (B) Schematic side view of the device showing neurons plated on bare and LbL (PLL/PLGA) surfaces. (C) Quantification of the surfaces showing the distinct populations of neurons which were differentiated (neurons vs astrocytes), showing that the LbL-coated surfaces along with direct stimulation from the ITO allows for controlled differentiation into mainly neurons ( $n = 8$ ) or a coculture with 50:50 differentiation with PLL and direct stimulation. NSPCs cultured on bare ITO glass with (D) 40 and (E) 80 mV electrical stimulation. Anti-MAP2 staining is in green (neurons) while anti-GFAP staining is in blue (astrocytes). NSPCs cultured on PLL/PLGA on ITO-glass with (F) 7.5 and (G) 8 layers. This demonstrates how critical the LbL surface is for the differentiation of neurons from NSPCs. Adapted from Lei et al.<sup>112</sup> with permission from the American Chemical Society, *Langmuir*. Copyright 2014.

capacity to fine tune surface properties postproduction and can limit some of the applications for biomedical devices. LbL material can have dramatically different surface properties under direct electrical stimulation, thus the approach using a combination of an LbL-assembled surface in conjunction with direct electrical stimulation may be used to tune the surface properties of a coating postproduction.<sup>110,111</sup> In fact, neural stem cell differentiation can be induced by surface properties and also by electrical stimulation. Lei and co-workers recently reported successfully controlling the differentiation of neural stem cells into functional neurons using an LbL-assembled PLL/PLGA film along with direct electrical stimulation.<sup>112</sup> Films were layered on an indium tin oxide (ITO) substrate (a clear semiconductor, Figure 13A,B), and a microfluidic system was then built on top. By controlling the electrical stimulation, neural stem cells were differentiated and the neurite extension was assayed.<sup>112</sup> Following 80 mV electrical stimulation for 3 days, uniaxial neurite extension was achieved, with some processes extending well beyond 300  $\mu\text{m}$ .<sup>112</sup> These findings demonstrate the capacity to apply an external stimulus to tailor a surface's properties, postproduction, and thereby elicit a specific cellular response (Figure 13C–G).

Finally, in a paper utilizing poly- $\epsilon$ -caprolactone spun nanofibrous scaffolds for culturing primary cortical neurons, Zhou et al. demonstrated that LbL coatings do not impede electrical conductivity.<sup>113</sup> By using a highly engineered graphene-heparin/

PLL system to coat the complex nanofibrous scaffold, an electrically active yet neurally permissive scaffold was created. Graphene was chosen to impart electrical conductivity, while PLL was used to promote neural cell adhesion to the scaffold. This electrically active yet neural cell culture permissive scaffold was found to perform similarly to PLL surfaces while not impeding electrical conductivity, opening possibilities for electrically active coatings that direct neurite growth.<sup>113</sup> Zhou and co-workers were able to demonstrate substantial neurite outgrowth on their modified scaffolds, which did not differ statistically from graphene-free surfaces ( $61 \pm 6 \mu\text{m}$ ), providing that graphene is permissive for neuronal growth and development.<sup>113</sup>

#### Making Wet in Situ Measurements of These Layers.

Toward the aim of the rational development of new coatings, it is essential to elucidate structure–performance relationships between what can be measured and known about the physicochemical properties of the polymer layers and multilayers and the response of the cells in culture. It is thus essential to be able to make measurements of the relevant properties in situ—in the wet biological environment in which the coatings will be applied as opposed to dry and cold, the usual standard conditions of traditional experimental physical chemistry. Historically, observing in situ has involved adapting the set of characterization tools typically used by spectroscopists to accommodate conditions more typical of living cells (i.e., performing the

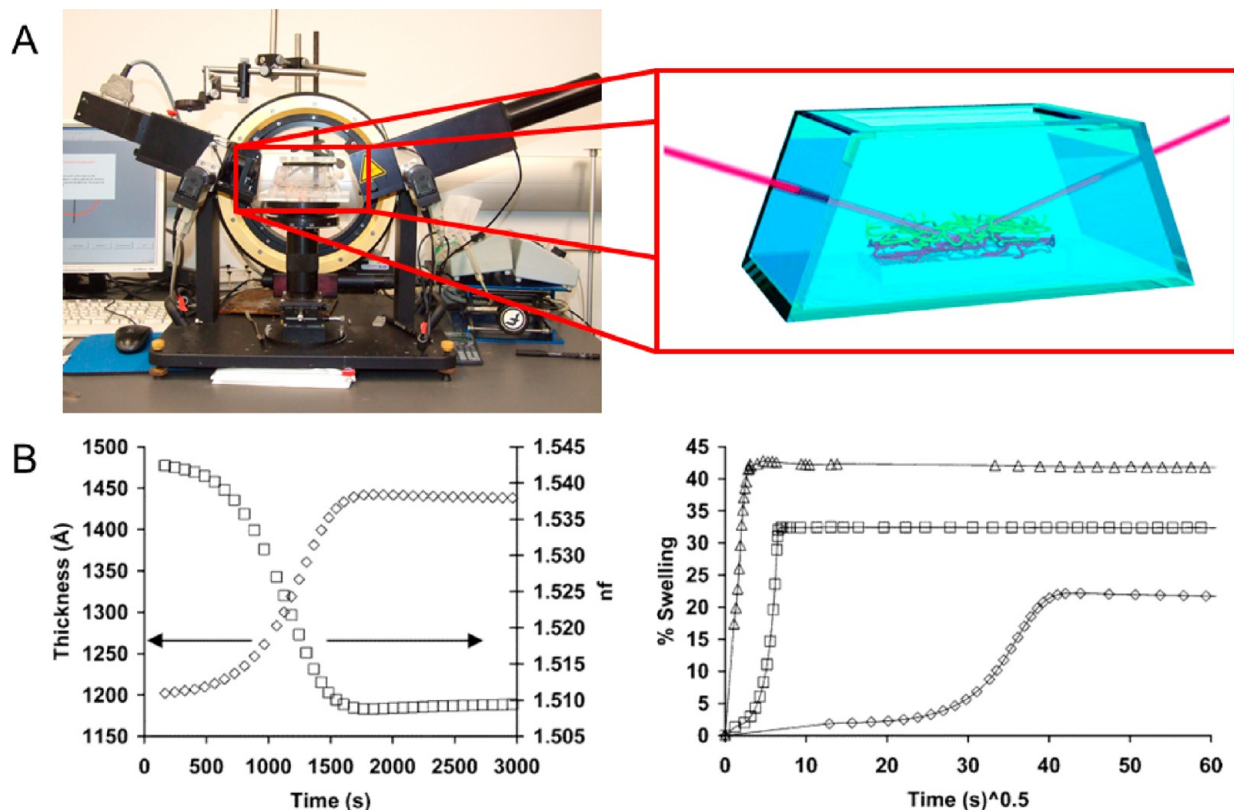


**Figure 14.** (A) Setup for in situ swelling measurement of the thickness ( $h$ ) and refractive index of a film ( $nf$ ) of LbL-deposited polymers (PAH/PAA) with (left) a modified ellipsometer. (Right) Schematic drawing of the liquid sample cell with the probe laser beam interfering with the LbL polymer surface underwater to measure  $h$  and  $nf$ . (B, left) Curve showing a PAH/PAA surface (25 bilayers) swelling underwater from time = 0. The thickness increases by 20% (diamonds), and the refractive index decreases proportionally (squares). (B, right) Demonstration of the vast difference (logarithmic scale) in swelling rate when PAH/PAA films are assembled under different pH conditions and with a different number of layers. Twenty-five bilayers, pH = 3.5 ( $\diamond$ ); 15 bilayers, pH = 5.0 ( $\square$ ); and 60 bilayers, pH = 6.5 ( $\triangle$ ). Adapted from Tanchak et al.<sup>120</sup> with permission from the American Chemical Society, *Chem. Mater.* Copyright 2014.

characterization experiments in as close to a real biological environment as possible), at a minimum in equilibrium completely underwater and better yet at biological temperatures and in cell culture media if possible. Two of the key properties that need to be accurately measured are the water content in the layers and the stiffness. Other mechanical properties can also be of relevance, as well as the ion content and distribution and knowing the acid–base and other dynamic equilibria in the coatings, which can often be markedly different than in dilute solution. In general, the “wetter” and the “softer”, the better, which also creates additional challenges as more sensitive measurements are often required than are typical.

Measurements of the modulus are perhaps the most easily performed, as it has generally been fairly straightforward to adapt commercial nanoindentation tools to run in a liquid cell.<sup>114</sup> For more delicate measurements of coatings thinner than 1  $\mu\text{m}$  and/or soft moduli in the range of Pascals, more sensitive Atomic Force microscopes (AFM) can be used in force–distance mode and underwater, and reasonable estimates of very soft moduli could be extracted statistically from many hundreds of indentations.<sup>115</sup> This AFM force–distance technique has the added benefit of the ability to record adhesion events during the tip retraction phase and thus to measure surface “stickiness” at the same time if the AFM tip is also coated with cell-like LbL coatings.<sup>115</sup> In an experimental configuration already discussed for high-throughput combinatorial gradient 1-D and 2-D coating studies, one can simply automate the indent/retraction data

collection concurrent with an  $x$ – $y$  repositionable sample stage so that separate measurements spaced as closely as 1 mm apart can be made independently, and up to 10 000 such separate modulus measurements have been demonstrated in a 2-D 10 cm  $\times$  10 cm film.<sup>25</sup>

Toward the development of coatings which are as stable as possible to desorption or rearrangement over time, it is also important to be able to characterize any dynamic equilibria that the coatings might form with the surrounding media, such as acid–base protonation or deprotonation. While direct measurement of this acid–base equilibria on cell culture surfaces is quite challenging, one can instead get adequate results from an analogous model system where the coatings are applied to small spherical nanoparticles of the same underlying substrate chemistries (silicates, plastics, etc.) and then use electrophoresis to measure the zeta potential charge of the surface.<sup>93,116</sup> Making this measurement in a series of different pH environments allows one to construct a surface charge vs pH plot to determine an apparent  $\text{p}K_a$  or  $\text{p}K_b$  of the polymer coatings from the inflection points, which can be substantially different (1–3 log units) from the  $\text{p}K_a$  and  $\text{p}K_b$  values of the same polymers in dilute solution. This provides insight toward what rearrangements and equilibria might be expected at pH 7.4 in the cell culture and rationalizes many physicochemical properties that can be strongly non-equilibrium.<sup>117</sup>

The same layering-onto-nanoparticle approach can be used to take advantage of high surface-to-volume ratios of the small



systems, to permit bulk measurements to be applied to coatings of tens of nanometers or even less, for example, by solid-state NMR spectroscopy.<sup>118,119</sup> These sensitive NMR measurements can confirm internal bonding arrangements of polymer multilayer assemblies and the structural composition, if unknown, via either the proton<sup>118</sup> or carbon signals.<sup>119</sup> Furthermore, solid-state NMR can also yield information on the amount of water that is contained in the layers,<sup>119</sup> although this is not a true in situ measurement.

In order to make a true wet in situ measurement of the water content of the real (flat, not spherical model) coatings, in as close an approximation as possible to the environment experienced in cell culture media, gentle radiation reflection techniques can be employed, such as ellipsometry, surface plasmon resonance spectroscopy, and neutron reflectometry.<sup>28,120–123</sup> One simply needs to replace the instrument's dry sample holder with a liquid-holding cell with windows transparent to the radiation wavelengths employed and to reprogram the analysis and interpretation software to model the ambient medium as the refractive index properties of water and not air. This can be accomplished most simply with a commercial ellipsometer,<sup>120,121</sup> with a home-built liquid sample holder with transparent and nonbirefringent windows, aligned normal to the incident and output laser beams (Figure 14A).<sup>120</sup> The cell can even be brought to biological temperature, and more representative environments such as cell culture media can be used instead of water, as long as they are transparent in the visible spectrum and the refractive index and extinction coefficients are known. Here, one measures the thickness and refractive index independently when wet, and compared to the known initial thickness and refractive index of the same coating in the dry state, this implies how much water penetrated to both increase the thickness and dilute the refractive index proportionally. Since measurements can be collected once per second or faster, this also permits real-time tracking of the dynamics of water swelling from dry to hydrated over seconds, minutes, or hours (Figure 14B). In order to confirm these measurements by an independent and more powerful technique, a similar liquid cell can be home-built for variable-angle neutron reflectometry,<sup>122</sup> where now any gradients in film composition can also be observed, in addition to confirming the results obtained by ellipsometry.<sup>25</sup> Good correlation was demonstrated by the two independent techniques, water content levels from 5% to more than 80% could be measured, and coating fabrication protocols could be developed to tune the water content to the desired intermediate values. Gradients of the water profile throughout the coating and the distribution of ions can also be ascertained by neutron reflectometry.<sup>123</sup>

**Dynamic Systems for Next-Generation Active Surfaces.** LbL thin films offer a versatile tool to functionalize surfaces and create soft yet stable material coatings specifically aimed at mimicking neural ECM to create surfaces that support neuronal survival and growth. Control over the physical properties of a LbL film can be achieved during the process of deposition, effectively locking in any physical property, such as the modulus, created by the depositing process. Future research directions toward permitting dynamic properties that can be postmodified or postprocessed have been described that create reversible, stimuli-responsive, and externally addressable systems. Work reported by Wang et al. has presented an LbL thin film system with a dynamic stiffness based on labile disulfide bonds that allow control of cell morphology and adhesion through chemical means.<sup>85</sup> While this work does allow for precise control over the

material's moduli, we believe the most promising future systems will be controlled through external, localized, and noninterfering stimuli, not chemically. One such way to create an externally addressable system is through the addition of photoswitchable molecules, such as azobenzene, within a material.

Chromophores, such as azobenzene, can be added to the LbL assembly process through chemical means<sup>124</sup> or through soft bonds.<sup>125</sup> The addition of photoswitches to biologically relevant polymers creates new biomaterials that exhibit optical properties while remaining biologically permissive. This provides biomaterials that are (1) externally addressable, (2) allow the experimenter to change/tune material properties in vitro and on the fly, and (3) allow localized control of cell biology through single-cell switching (i.e., light can modify the surface around a single cell and tune its properties relative to others around it). Published reviews have highlighted the use of such chromophores in biological systems for cellular control and sensing.<sup>126,127</sup> Polymers have been previously created with photo-responsive moieties as pendant groups and were demonstrated to allow for the explicit control of the modulus and surface topology using laser irradiation as an external stimulus.<sup>128</sup> Azobenzene in particular is a dominant class of photoisomerizing dyes that possess the ability to switch reversibly and quickly between distinct trans and cis geometries upon the absorption of low-power light of the appropriate wavelength, including low-biointerfering visible regions. Azo groups can also be copolymerized with polyelectrolytes and assembled into thin film architectures to achieve similar control over surface energy as demonstrated by Sailer et al., who reported the use of disperse red 2 dye copolymerized with poly(acrylic acid) (DR2-co-PAA).<sup>129</sup> A 10% loading of the azo dye was sufficient to induce molecular orientation, and for the first time, resulting birefringence was measured and determined to be stable when completely under water, demonstrating that azobenzene can photoswitch and orient completely under water, extending its application potentials as externally and locally addressable biomaterials.<sup>129</sup>

More complex photoswitches can be functionalized into LbL systems to allow new avenues for targeted cellular control. Work by Goulet-Hanssens et al. achieved dynamic control of cell adhesion when incorporating an azobenzene switch functionalized with a cyclic RGD peptide as a cell adhesive (Figure 15).<sup>127</sup>

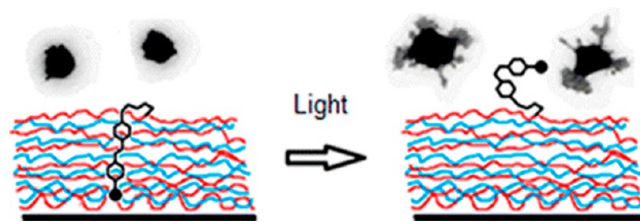


**Figure 15.** Schematic representation of a multilayer containing an azobenzene-functionalized cyclic RGD that allows for photocontrol over the adhesion of NIH 3T3 cells on the surface. Reprinted from Goulet-Hanssens et al.<sup>127</sup> with permission from the American Chemical Society, *Biomacromolecules*. Copyright 2012.

Low concentrations of dye of below 1% were sufficient to control the adhesion of neural cells onto the LbL surface,<sup>127</sup> demonstrating in principle that light-responsive biomaterials can be capable of direct control over cellular function.

LbL assemblies with azobenzene have demonstrated the power of externally addressable biomaterials and the possibility

to influence and dynamically control biological systems. Silk can also be modified with azobenzene chemically to create a dynamic biomaterial that is photoresponsive. This new material has been called azosilk or opto-silk, and it combines the utility of azobenzene photoreversible dyes with the natural biomaterial properties of silk.<sup>130</sup> While the majority of the previous applications of azosilk used the process of azobenzene functionalization as a means to tune the surface properties chemically, Landry et al. used azosilk as a means to achieve dynamic control of the topology and modulus of the surface using light as an external stimulus.<sup>59</sup> Upon exposure to 800 nm light, these silk surfaces expand and bubble and can thus be patterned. The irradiated surface bubbles exhibit a greater than 10-fold decrease in modulus (from 12 to 0.6 kPa).<sup>59</sup> This has the potential to locally manipulate cells by modifying the physical properties of the underlying growth substrate actively with light postplating, in an active cell culture medium, for the potential application of guiding the migration of modulus-sensitive cells such as neurons as they grow and interact.

## CONCLUSIONS

Throughout this literature review, we have identified a convergence of the field addressing artificial ECM materials toward developing materials that are bioinspired, self-assembled through dynamic bonds, soft, and contain high amounts of water. The reports described demonstrate these guiding principles for developing enhanced methods to cultivate and study neurons using more complex and sophisticated means. Remarkably, some of the materials first used by Harrison's pioneering work on neurite outgrowth in 1914 used biologically sourced spider silk, and 100 years later, the field has returned to silk as a promising material of the future. Polymer chemists over the past 60 years have indeed provided novel new materials but also traditional ones that are hard, built from nonbiological (foreign) chemical functionalities, while naturally derived polymers optimized through evolutionary processes have been harvested and postengineered by humans for thousands of years. These biologically sourced and neurologically supportive materials may be a challenge to work with, yet we anticipate that the field can create highly viable and biologically supportive materials by taking inspiration from the structures and functionalities of complex natural materials. We believe that the design principles outlined here illustrate not only a growing trend of success achieved within the community toward developing and applying new and superior artificial ECM coating materials but also an inspiring guide for future experimenters to pay attention to nature for the creation of next-generation materials for interfacing with neural cells and other fronts of the biointerface.

## AUTHOR INFORMATION

### Corresponding Authors

\*E-mail: [timothy.kennedy@mcgill.ca](mailto:timothy.kennedy@mcgill.ca).

\*E-mail: [christopher.barrett@mcgill.ca](mailto:christopher.barrett@mcgill.ca).

### ORCID

Christopher J. Barrett: 0000-0001-6194-9066

### Funding

M.J.L. was supported by grants from the Collaborative Health Research Program (CHRP) of the Canadian Institutes of Health Research (CIHR 357055) and from the Natural Sciences and Engineering Research Council of Canada (NSERC 493633-16).

### Notes

The authors declare no competing financial interest.

## Biography



Michael J. Landry (center right) and Frédéric-Guillaume Rollet (center left) authored this review as graduate students at McGill University, working with Professors Christopher J. Barrett in Chemistry (left) and Timothy E. Kennedy (right) of the adjacent Montreal Neurological Institute. Landry earned a B.Sc. in chemistry from the University of New Brunswick Canada, and Rollet holds B.Sc. and M.Sc. degrees from the University of Montreal. Christopher J. Barrett joined McGill Chemistry in 2000, after a Ph.D. in Chemistry at Queen's University Canada with Almeria Natansohn on light-responsive polymers and then postdoctoral work at MIT with Anne Mayes and Michael Rubner on self-assembled polymer coatings and biocompatible surfaces. Timothy E. Kennedy joined the Montreal Neurological Institute and Hospital in 1996, following a Ph.D. in physiology and biophysics from Columbia University with Eric Kandel investigating the molecular mechanisms that underlie learning and memory and postdoctoral research at UC San Francisco with Marc Tessier-Lavigne, addressing the mechanisms that direct axon guidance during embryogenesis. Barrett and Kennedy have enjoyed a successful scientific collaboration for the past decade between their institutes in Montreal, sharing grants and students and coauthoring papers on understanding and manipulating neural cell–surface interactions.

## ACKNOWLEDGMENTS

T.E.K. and C.J.B. are grateful to the NSERC CREATE program (Canada), which funded the interdisciplinary collaboration on neuroengineering research between the MNI and the McGill Faculty of Science.

## ABBREVIATIONS

1-D, one-dimensional; 2-D, two-dimensional; 3-D, three-dimensional; AFM, atomic force microscope; BDNF, brain-derived neurotrophic factor; BMP-2, bone morphogenetic protein 2; CNS, central nervous system; DR2-co-PAA, disperse red 2 copolyacrylic acid; DRG, dorsal root ganglion; ECM, extracellular matrix; GDNF, glial cell line-derived neurotrophic factor; GFAP, glial fibrillary acidic protein; HA, hyaluronic acid; ITO, indium tin oxide; LbL, layer-by-layer; MAP, microtubule-associated protein 2; N52, neurofilament antibody reacting with the 200 side arm; NGF, nerve growth factor; NIH 3T3, National Institutes of Health 3-day-transfer mouse embryonic fibroblast cell line; NPC, neural progenitor cell; NSPC, neural stem and progenitor cell; PAA, poly(acrylic acid); PAH, poly(allylamine hydrochloride); PDAC, poly(diallyldimethylammonium chloride); PDL, poly-D-lysine; PE, polyelectrolyte; PEDOT, poly(3,4-ethylenedioxythiophene); PEM, polyelectrolyte multilayer; PLGA, poly(L-glutamic acid); PLL, poly-L-lysine; PNS, peripheral nervous system; PSS, poly(styrenesulfonate); SPS, sulfonated polystyrene; RGD, arginylglycylaspartic acid; SC, Schwann cells; SF, silk fibroin

## REFERENCES

(1) Hynes, R. O.; Yamada, K. M. *Extracellular Matrix Biology*; Cold Spring Harbor Laboratory Press: Cold Spring Harbor, New York, 2012.

- (2) Hynes, R. O. Integrins: a family of cell surface receptors. *Cell* **1987**, *48* (4), 549–554.
- (3) Lutolf, M. P.; Hubbell, J. A. Synthetic biomaterials as instructive extracellular microenvironments for morphogenesis in tissue engineering. *Nat. Biotechnol.* **2005**, *23* (1), 47–55.
- (4) Lee, I. C.; Wu, Y. C.; Cheng, E. M.; Yang, W. T. Biomimetic niche for neural stem cell differentiation using poly-L-lysine/hyaluronic acid multilayer films. *J. Biomater. Appl.* **2015**, *29* (10), 1418–1427.
- (5) Suri, S.; Schmidt, C. E. Cell-laden hydrogel constructs of hyaluronic acid, collagen, and laminin for neural tissue engineering. *Tissue Eng., Part A* **2010**, *16* (5), 1703–1716.
- (6) Wei, K.; Kim, B. S.; Kim, I. S. Fabrication and biocompatibility of electrospun silk biocomposites. *Membranes (Basel, Switz.)* **2011**, *1* (4), 275–298.
- (7) Gao, M.; Tao, H.; Wang, T.; Wei, A.; He, B. Functionalized self-assembly polypeptide hydrogel scaffold applied in modulation of neural progenitor cell behavior. *J. Bioact. Compat. Polym.* **2017**, *32* (1), 45–60.
- (8) Maniotis, A. J.; Folberg, R.; Hess, A.; Seftor, E. A.; Gardner, L. M.; Pe'er, J.; Trent, J. M.; Meltzer, P. S.; Hendrix, M. J. Vascular channel formation by human melanoma cells *in vivo* and *in vitro*: vasculogenic mimicry. *Am. J. Pathol.* **1999**, *155* (3), 739–752.
- (9) Karp, G. *Cell and Molecular Biology: Concepts and Experiments*, 4th ed.; John Wiley & Son: Hoboken, NJ, 2006.
- (10) Kandel, E. R.; Schwartz, J. H.; Jessell, T. M. *Principles of Neural Science*, 4th ed.; McGraw-Hill: New York, 2000.
- (11) Yates, D. Neurodegenerative disease: neurodegenerative networking. *Nat. Rev. Neurosci.* **2012**, *13* (5), 288–289.
- (12) Millet, L. J.; Gillette, M. U. Over a century of neuron culture: from the hanging drop to microfluidic devices. *Yale J. Biol. Med.* **2012**, *85* (4), 501–521.
- (13) Harrison, R. G. The reaction of embryonic cells to solid structures. *J. Exp. Zool.* **1914**, *17* (4), 521–544.
- (14) Leipzig, N. D.; Shoichet, M. S. The effect of substrate stiffness on adult neural stem cell behavior. *Biomaterials* **2009**, *30* (36), 6867–6878.
- (15) Wang, H.-B.; Dembo, M.; Wang, Y.-L. Substrate flexibility regulates growth and apoptosis of normal, untransformed cells. *Am. J. Physiol., Cell Physiol.* **2000**, *279* (5), C1345–C1350.
- (16) Yeung, T.; Georges, P. C.; Flanagan, L. A.; Marg, B.; Ortiz, M.; Funaki, M.; Zahir, N.; Ming, W.; Weaver, V.; Janmey, P. A. Effects of substrate stiffness on cell morphology, cytoskeletal structure, and adhesion. *Cell Motil. Cytoskeleton* **2005**, *60* (1), 24–34.
- (17) He, Y. X.; Zhang, N. N.; Li, W. F.; Jia, N.; Chen, B. Y.; Zhou, K.; Zhang, J.; Chen, Y.; Zhou, C. Z. N-terminal domain of *Bombyx mori* fibroin mediates the assembly of silk in response to pH decrease. *J. Mol. Biol.* **2012**, *418* (3), 197–207.
- (18) Farhat, T.; Yassin, G.; Dubas, S. T.; Schlenoff, J. B. Water and ion pairing in polyelectrolyte multilayers. *Langmuir* **1999**, *15* (20), 6621–6623.
- (19) Rodríguez-Lozano, F. J.; García-Bernal, D.; Aznar-Cervantes, S.; Ros-Roca, M. A.; Algueró, M. C.; Atucha, N. M.; Lozano-García, A. A.; Moraleda, J. M.; Cenis, J. L. Effects of composite films of silk fibroin and graphene oxide on the proliferation, cell viability and mesenchymal phenotype of periodontal ligament stem cells. *J. Mater. Sci.: Mater. Med.* **2014**, *25* (12), 2731–2741.
- (20) Banerjee, A.; Arha, M.; Choudhary, S.; Ashton, R. S.; Bhatia, S. R.; Schaffer, D. V.; Kane, R. S. The influence of hydrogel modulus on the proliferation and differentiation of encapsulated neural stem cells. *Biomaterials* **2009**, *30* (27), 4695–4699.
- (21) Saha, K.; Keung, A. J.; Irwin, E. F.; Li, Y.; Little, L.; Schaffer, D. V.; Healy, K. E. Substrate modulus directs neural stem cell behavior. *Biophys. J.* **2008**, *95* (9), 4426–4438.
- (22) Levental, I.; Georges, P. C.; Janmey, P. A. Soft biological materials and their impact on cell function. *Soft Matter* **2007**, *3* (3), 299–306.
- (23) Sailer, M.; Lai Wing Sun, K.; Mermut, O.; Kennedy, T. E.; Barrett, C. J. High-throughput cellular screening of engineered ECM based on combinatorial polyelectrolyte multilayer films. *Biomaterials* **2012**, *33* (24), 5841–5847.
- (24) Georges, P. C.; Janmey, P. A. Cell type-specific response to growth on soft materials. *J. Appl. Physiol.* **2005**, *98* (4), 1547–1553.
- (25) Sailer, M.; Barrett, C. J. Fabrication of two-dimensional gradient layer-by-layer films for combinatorial biosurface studies. *Macromolecules* **2012**, *45* (14), 5704–5711.
- (26) Wang, Q.; Mynar, J. L.; Yoshida, M.; Lee, E.; Lee, M.; Okuro, K.; Kinbara, K.; Aida, T. High-water-content mouldable hydrogels by mixing clay and a dendritic molecular binder. *Nature* **2010**, *463* (7279), 339–343.
- (27) Su, D.; Yao, M.; Liu, J.; Zhong, Y.; Chen, X.; Shao, Z. Enhancing mechanical properties of silk fibroin hydrogel through restricting the growth of  $\beta$ -Sheet domains. *ACS Appl. Mater. Interfaces* **2017**, *9* (20), 17489–17498.
- (28) Tanchak, O. M.; Yager, K. G.; Fritzsche, H.; Harroun, T.; Katsaras, J.; Barrett, C. J. Water distribution in multilayers of weak polyelectrolytes. *Langmuir* **2006**, *22* (11), 5137–5143.
- (29) Jordan, J.; Jacob, K. I.; Tannenbaum, R.; Sharaf, M. A.; Jasiuk, I. Experimental trends in polymer nanocomposites—a review. *Mater. Sci. Eng., A* **2005**, *393* (1), 1–11.
- (30) Kolacna, L.; Bakesova, J.; Varga, F.; Kostakova, E.; Planka, L.; Necas, A.; Lukas, D.; Amler, E.; Pelouch, V. Biochemical and biophysical aspects of collagen nanostructure in the extracellular matrix. *Physiol. Res.* **2007**, *56*, 51–60.
- (31) Georges, P. C.; Miller, W. J.; Meaney, D. F.; Sawyer, E. S.; Janmey, P. A. Matrices with compliance comparable to that of brain tissue select neuronal over glial growth in mixed cortical cultures. *Biophys. J.* **2006**, *90* (8), 3012–3018.
- (32) Zhang, Q.; Zhao, Y.; Yan, S.; Yang, Y.; Zhao, H.; Li, M.; Lu, S.; Kaplan, D. L. Preparation of uniaxial multichannel silk fibroin scaffolds for guiding primary neurons. *Acta Biomater.* **2012**, *8* (7), 2628–2638.
- (33) Kundu, B.; Kurland, N. E.; Bano, S.; Patra, C.; Engel, F. B.; Yadavalli, V. K.; Kundu, S. C. Silk proteins for biomedical applications: bioengineering perspectives. *Prog. Polym. Sci.* **2014**, *39* (2), 251–267.
- (34) Li, Z.-H.; Ji, S.-C.; Wang, Y.-Z.; Shen, X.-C.; Liang, H. Silk fibroin-based scaffolds for tissue engineering. *Front. Mater. Sci.* **2013**, *7* (3), 237–247.
- (35) Ghezzi, C. E.; Rnjak-Kovacic, J.; Weiss, A. S.; Kaplan, D. L. Multifunctional silk-tropoelastin biomaterial systems. *Isr. J. Chem.* **2013**, *53* (9), 777–786.
- (36) Volkov, V.; Ferreira, A. V.; Cavaco-Paulo, A. On the routines of wild-type silk fibroin processing toward silk-inspired materials: a review. *Macromol. Mater. Eng.* **2015**, *300* (12), 1199–1216.
- (37) Asakura, T.; Yao, J.; Yamane, T.; Umemura, K.; Ulrich, A. S. Heterogeneous structure of silk fibers from *Bombyx mori* resolved by  $^{13}\text{C}$  solid-state NMR spectroscopy. *J. Am. Chem. Soc.* **2002**, *124* (30), 8794–8795.
- (38) Yan, L. P.; Oliveira, J. M.; Oliveira, A. L.; Caridade, S. G.; Mano, J. F.; Reis, R. L. Macro/microporous silk fibroin scaffolds with potential for articular cartilage and meniscus tissue engineering applications. *Acta Biomater.* **2012**, *8* (1), 289–301.
- (39) Freddi, G.; Pessina, G.; Tsukada, M. Swelling and dissolution of silk fibroin (*Bombyx mori*) in N-methyl morpholine N-oxide. *Int. J. Biol. Macromol.* **1999**, *24* (2), 251–263.
- (40) Rockwood, D. N.; Preda, R. C.; Yucel, T.; Wang, X.; Lovett, M. L.; Kaplan, D. L. Materials fabrication from *Bombyx mori* silk fibroin. *Nat. Protoc.* **2011**, *6* (10), 1612–1631.
- (41) Ude, A. U.; Eshkoo, R. A.; Zulkifli, R.; Ariffin, A. K.; Dzuraidah, A. W.; Azhari, C. H. *Bombyx mori* silk fibre and its composite: a review of contemporary developments. *Mater. Eng.* **2014**, *57*, 298–305.
- (42) Servoli, E.; Maniglio, D.; Motta, A.; Predazzer, R.; Migliaresi, C. Surface properties of silk fibroin films and their interaction with fibroblasts. *Macromol. Biosci.* **2005**, *5* (12), 1175–1183.
- (43) Huang, W.; Begum, R.; Barber, T.; Ibba, V.; Tee, N. C.; Hussain, M.; Arastoo, M.; Yang, Q.; Robson, L. G.; Lesage, S.; Gheysens, T.; Skaer, N. J.; Knight, D. P.; Priestley, J. V. Regenerative potential of silk conduits in repair of peripheral nerve injury in adult rats. *Biomaterials* **2012**, *33* (1), 59–71.
- (44) Wang, Z.; Park, J. H.; Park, H. H.; Tan, W.; Park, T. H. Enhancement of recombinant human EPO production and sialylation in chinese hamster ovary cells through *Bombyx mori* 30Kc19 gene expression. *Biotechnol. Bioeng.* **2011**, *108* (7), 1634–1642.

- (45) Young, E. W.; Wheeler, A. R.; Simmons, C. A. Matrix-dependent adhesion of vascular and valvular endothelial cells in microfluidic channels. *Lab Chip* **2007**, *7* (12), 1759–1766.
- (46) Patra, C.; Talukdar, S.; Novoyatleva, T.; Velagala, S. R.; Muhlfield, C.; Kundu, B.; Kundu, S. C.; Engel, F. B. Silk protein fibroin from *Antheraea mylitta* for cardiac tissue engineering. *Biomaterials* **2012**, *33* (9), 2673–2680.
- (47) Yang, Y.; Chen, X.; Ding, F.; Zhang, P.; Liu, J.; Gu, X. Biocompatibility evaluation of silk fibroin with peripheral nerve tissues and cells *in vitro*. *Biomaterials* **2007**, *28* (9), 1643–1652.
- (48) Tang, X.; Ding, F.; Yang, Y.; Hu, N.; Wu, H.; Gu, X. Evaluation on *in vitro* biocompatibility of silk fibroin-based biomaterials with primarily cultured hippocampal neurons. *J. Biomed. Mater. Res., Part A* **2009**, *91* (1), 166–174.
- (49) Lecomte, A.; Degache, A.; Descamps, E.; Dahan, L.; Bergaud, C. *In vitro* and *in vivo* biostability assessment of chronically-implanted parylene C neural sensors. *Sens. Actuators, B* **2017**, *251* (Supplement C), 1001–1008.
- (50) Xue, C.; Ren, H.; Zhu, H.; Gu, X.; Guo, Q.; Zhou, Y.; Huang, J.; Wang, S.; Zha, G.; Gu, J.; Yang, Y.; Gu, Y.; Gu, X. Bone marrow mesenchymal stem cell-derived acellular matrix-coated chitosan/silk scaffolds for neural tissue regeneration. *J. Mater. Chem. B* **2017**, *5* (6), 1246–1257.
- (51) Gu, Y.; Zhu, J.; Xue, C.; Li, Z.; Ding, F.; Yang, Y.; Gu, X. Chitosan/silk fibroin-based, Schwann cell-derived extracellular matrix-modified scaffolds for bridging rat sciatic nerve gaps. *Biomaterials* **2014**, *35* (7), 2253–2263.
- (52) Teshima, T.; Nakashima, H.; Kasai, N.; Sasaki, S.; Tanaka, A.; Tsukada, S.; Sumitomo, K. Mobile silk fibroin electrode for manipulation and electrical stimulation of adherent cells. *Adv. Funct. Mater.* **2016**, *26* (45), 8185–8193.
- (53) Gupta, M. K.; Khokhar, S. K.; Phillips, D. M.; Sowards, L. A.; Drummy, L. F.; Kadakia, M. P.; Naik, R. R. Patterned silk films cast from ionic liquid solubilized fibroin as scaffolds for cell growth. *Langmuir* **2007**, *23* (3), 1315–1319.
- (54) Beh, W. S.; Kim, I. T.; Qin, D.; Xia, Y.; Whitesides, G. M. Formation of patterned microstructures of conducting polymers by soft lithography, and applications in microelectronic device fabrication. *Adv. Mater.* **1999**, *11* (12), 1038–1041.
- (55) Tan, F.; Walshe, P.; Viani, L.; Al-Rubeai, M. Surface biotechnology for refining cochlear implants. *Trends Biotechnol.* **2013**, *31* (12), 678–687.
- (56) Zhu, W.; O'Brien, C.; O'Brien, J. R.; Zhang, L. G. 3D nano/microfabrication techniques and nanobiomaterials for neural tissue regeneration. *Nanomedicine (London, U. K.)* **2014**, *9* (6), 859–875.
- (57) Perry, H.; Gopinath, A.; Kaplan, D. L.; Dal Negro, L.; Omenetto, F. G. Nano- and Micropatterning of optically transparent, mechanically robust, biocompatible silk fibroin films. *Adv. Mater.* **2008**, *20* (16), 3070–3072.
- (58) Galeotti, F.; Andicsova, A.; Yunus, S.; Botta, C. Precise surface patterning of silk fibroin films by breath figures. *Soft Matter* **2012**, *8* (17), 4815–4821.
- (59) Landry, M. J.; Applegate, M. B.; Bushuyev, O. S.; Omenetto, F. G.; Kaplan, D. L.; Cronin-Golomb, M.; Barrett, C. J. Photo-induced structural modification of silk gels containing azobenzene side groups. *Soft Matter* **2017**, *13* (16), 2903–2906.
- (60) Hronik-Tupaj, M.; Raja, W. K.; Tang-Schomer, M.; Omenetto, F. G.; Kaplan, D. L. Neural responses to electrical stimulation on patterned silk films. *J. Biomed. Mater. Res., Part A* **2013**, *101* (9), 2559–2572.
- (61) Byette, F.; Bouchard, F.; Pellerin, C.; Paquin, J.; Marcotte, I.; Mateescu, M. A. Cell-culture compatible silk fibroin scaffolds concomitantly patterned by freezing conditions and salt concentration. *Polym. Bull.* **2011**, *67* (1), 159–175.
- (62) Lucido, A. L.; Suarez Sanchez, F.; Thostrup, P.; Kwiatkowski, A. V.; Leal-Ortiz, S.; Gopalakrishnan, G.; Liazoghli, D.; Belkaid, W.; Lennox, R. B.; Grutter, P.; Garner, C. C.; Colman, D. R. Rapid assembly of functional presynaptic boutons triggered by adhesive contacts. *J. Neurosci.* **2009**, *29* (40), 12449–12466.
- (63) Madduri, S.; Papaloizos, M.; Gander, B. Trophically and topographically functionalized silk fibroin nerve conduits for guided peripheral nerve regeneration. *Biomaterials* **2010**, *31* (8), 2323–2334.
- (64) Hopkins, A. M.; De Laporte, L.; Tortelli, F.; Spedden, E.; Staii, C.; Atherton, T. J.; Hubbell, J. A.; Kaplan, D. L. Silk hydrogels as soft substrates for neural tissue engineering. *Adv. Funct. Mater.* **2013**, *23* (41), 5140–5149.
- (65) Yao, M.; Zhou, Y.; Xue, C.; Ren, H.; Wang, S.; Zhu, H.; Gu, X.; Gu, X.; Gu, J. Repair of rat sciatic nerve defects by using allogeneic bone marrow mononuclear cells combined with chitosan/silk fibroin scaffold. *Cell Transplant.* **2016**, *25* (5), 983–993.
- (66) Bini, T. B.; Gao, S.; Xu, X.; Wang, S.; Ramakrishna, S.; Leong, K. W. Peripheral nerve regeneration by microbraided poly(L-lactide-co-glycolide) biodegradable polymer fibers. *J. Biomed. Mater. Res.* **2004**, *68* (2), 286–295.
- (67) Ren, Y. J.; Zhou, Z. Y.; Liu, B. F.; Xu, Q. Y.; Cui, F. Z. Preparation and characterization of fibroin/hyaluronic acid composite scaffold. *Int. J. Biol. Macromol.* **2009**, *44* (4), 372–378.
- (68) Tanaka, K.; Sata, M.; Komuro, I.; Saotome, T.; Yamashita, Y.; Asakura, T. P5377 Biodegradable extremely small diameter vascular graft made of silk fibroin leads rapid vascular remodeling; a preliminary evaluation. *Eur. Heart J.* **2017**, *38*, 1137.
- (69) Cai, Z.-X.; Mo, X.-M.; Zhang, K.-H.; Fan, L.-P.; Yin, A.-L.; He, C.-L.; Wang, H.-S. Fabrication of chitosan/silk fibroin composite nanofibers for wound-dressing applications. *Int. J. Mol. Sci.* **2010**, *11* (9), 3529–3539.
- (70) Schnell, E.; Klinkhammer, K.; Balzer, S.; Brook, G.; Klee, D.; Dalton, P.; Mey, J. Guidance of glial cell migration and axonal growth on electrospun nanofibers of poly- $\epsilon$ -caprolactone and a collagen/poly- $\epsilon$ -caprolactone blend. *Biomaterials* **2007**, *28* (19), 3012–3025.
- (71) Wei, Y.; Gong, K.; Zheng, Z.; Wang, A.; Ao, Q.; Gong, Y.; Zhang, X. Chitosan/silk fibroin-based tissue-engineered graft seeded with adipose-derived stem cells enhances nerve regeneration in a rat model. *J. Mater. Sci.: Mater. Med.* **2011**, *22* (8), 1947–1964.
- (72) Wang, C. Y.; Zhang, K. H.; Fan, C. Y.; Mo, X. M.; Ruan, H. J.; Li, F. F. Aligned natural-synthetic polyblend nanofibers for peripheral nerve regeneration. *Acta Biomater.* **2011**, *7* (2), 634–643.
- (73) Zhang, K.; Wang, H.; Huang, C.; Su, Y.; Mo, X.; Ikada, Y. Fabrication of silk fibroin blended P(LLA-CL) nanofibrous scaffolds for tissue engineering. *J. Biomed. Mater. Res., Part A* **2010**, *93* (3), 984–993.
- (74) Tang-Schomer, M. D.; White, J. D.; Tien, L. W.; Schmitt, L. I.; Valentin, T. M.; Graziano, D. J.; Hopkins, A. M.; Omenetto, F. G.; Haydon, P. G.; Kaplan, D. L. Bioengineered functional brain-like cortical tissue. *Proc. Natl. Acad. Sci. U. S. A.* **2014**, *111* (38), 13811–13816.
- (75) Ren, K.; Cruzier, T.; Roy, C.; Picart, C. Polyelectrolyte multilayer films of controlled stiffness modulate myoblast cells differentiation. *Adv. Funct. Mater.* **2008**, *18* (9), 1378–1389.
- (76) Decher, G.; Hong, J. D.; Schmitt, J. Buildup of ultrathin multilayer films by a self-assembly process: III. Consecutively alternating adsorption of anionic and cationic polyelectrolytes on charged surfaces. *Thin Solid Films* **1992**, *210-211*, 831–835.
- (77) Thebaud, N. B.; Bareille, R.; Daculsi, R.; Bourget, C.; Remy, M.; Kerdjoudj, H.; Menu, P.; Bordenave, L. Polyelectrolyte multilayer films allow seeded human progenitor-derived endothelial cells to remain functional under shear stress *in vitro*. *Acta Biomater.* **2010**, *6* (4), 1437–1445.
- (78) Richert, L.; Lavalle, P.; Vautier, D.; Senger, B.; Stoltz, J. F.; SchAAF, P.; Voegel, J. C.; Picart, C. Cell interactions with polyelectrolyte multilayer films. *Biomacromolecules* **2002**, *3* (6), 1170–1178.
- (79) Tsai, H. A.; Wu, R. R.; Lee, I. C.; Chang, H. Y.; Shen, C. N.; Chang, Y. C. Selection, enrichment, and maintenance of self-renewal liver stem/progenitor cells utilizing polypeptide polyelectrolyte multilayer films. *Biomacromolecules* **2010**, *11* (4), 994–1001.
- (80) Almodovar, J.; Bacon, S.; Gogolski, J.; Kisiday, J. D.; Kipper, M. J. Polysaccharide-based polyelectrolyte multilayer surface coatings can enhance mesenchymal stem cell response to adsorbed growth factors. *Biomacromolecules* **2010**, *11* (10), 2629–2639.
- (81) Jaklenec, A.; Anselmo, A. C.; Hong, J.; Vegas, A. J.; Kozminsky, M.; Langer, R.; Hammond, P. T.; Anderson, D. G. High throughput

- layer-by-layer films for extracting film forming parameters and modulating film interactions with cells. *ACS Appl. Mater. Interfaces* **2016**, *8* (3), 2255–2261.
- (82) Decher, G. Fuzzy nanoassemblies: toward layered polymeric multicomposites. *Science* **1997**, *277* (5330), 1232–1237.
- (83) Silva, J. M.; Reis, R. L.; Mano, J. F. Biomimetic extracellular environment based on natural origin polyelectrolyte multilayers. *Small* **2016**, *12* (32), 4308–4342.
- (84) Mendelsohn, J. D.; Yang, S. Y.; Hiller, J.; Hochbaum, A. I.; Rubner, M. F. Rational design of cytophilic and cytophobic polyelectrolyte multilayer thin films. *Biomacromolecules* **2003**, *4* (1), 96–106.
- (85) Wang, L.-M.; Chang, H.; Zhang, H.; Ren, K.-F.; Li, H.; Hu, M.; Li, B.-C.; Martins, M. C. L.; Barbosa, M. A.; Ji, J. Dynamic stiffness of polyelectrolyte multilayer films based on disulfide bonds for *in situ* control of cell adhesion. *J. Mater. Chem. B* **2015**, *3* (38), 7546–7553.
- (86) Thompson, M. T.; Berg, M. C.; Tobias, I. S.; Rubner, M. F.; Van Vliet, K. J. Tuning compliance of nanoscale polyelectrolyte multilayers to modulate cell adhesion. *Biomaterials* **2005**, *26* (34), 6836–6845.
- (87) Gribova, V.; Auzely-Velty, R.; Picart, C. Polyelectrolyte multilayer assemblies on materials surfaces: from cell adhesion to tissue engineering. *Chem. Mater.* **2012**, *24* (5), 854–869.
- (88) Borges, J.; Mano, J. F. Molecular interactions driving the layer-by-layer assembly of multilayers. *Chem. Rev.* **2014**, *114* (18), 8883–8942.
- (89) Sukhorukov, G. B.; Antipov, A. A.; Voigt, A.; Donath, E.; Möhwald, H. pH-controlled macromolecule encapsulation in and release from polyelectrolyte multilayer nanocapsules. *Macromol. Rapid Commun.* **2001**, *22* (1), 44–46.
- (90) Ai, H.; Jones, S. A.; Lvov, Y. M. Biomedical applications of electrostatic layer-by-layer nano-assembly of polymers, enzymes, and nanoparticles. *Cell Biochem. Biophys.* **2003**, *39* (1), 23–43.
- (91) Choy, K. L.; Schnabelrauch, M.; Wyrwa, R. Bioactive Coatings. In *Biomaterials in Clinical Practice: Advances in Clinical Research and Medical Devices*; Zivic, F., Affatato, S., Trajanovic, M., Schnabelrauch, M., Grujovic, N., Choy, K. L., Eds.; Springer International Publishing: Cham, Switzerland, 2018; pp 361–406.
- (92) Mermut, O.; Barrett, C. J. Effects of charge density and counterions on the assembly of polyelectrolyte multilayers. *J. Phys. Chem. B* **2003**, *107* (11), 2525–2530.
- (93) Burke, S. E.; Barrett, C. J. Acid–base equilibria of weak polyelectrolytes in multilayer thin films. *Langmuir* **2003**, *19* (8), 3297–3303.
- (94) Reyes, D. R.; Perruccio, E. M.; Becerra, S. P.; Locascio, L. E.; Gaitan, M. Micropatterning neuronal cells on polyelectrolyte multilayers. *Langmuir* **2004**, *20* (20), 8805–8811.
- (95) Zhou, K.; Sun, G. Z.; Bernard, C. C.; Thouas, G. A.; Nisbet, D. R.; Forsythe, J. S. Optimizing interfacial features to regulate neural progenitor cells using polyelectrolyte multilayers and brain derived neurotrophic factor. *Biointerphases* **2011**, *6* (4), 189–199.
- (96) Delcea, M.; Mohwald, H.; Skirtach, A. G. Stimuli-responsive LbL capsules and nanoshells for drug delivery. *Adv. Drug Delivery Rev.* **2011**, *63* (9), 730–747.
- (97) Luna-Acosta, J. L.; Alba-Betancourt, C.; Martínez-Moreno, C. G.; Ramírez, C.; Carranza, M.; Luna, M.; Arámburo, C. Direct antiapoptotic effects of growth hormone are mediated by PI3K/Akt pathway in the chicken bursa of Fabricius. *Gen. Comp. Endocrinol.* **2015**, *224* (Supplement C), 148–159.
- (98) Milkova, V.; Radeva, T. Influence of charge density and calcium salt on stiffness of polysaccharides multilayer film. *Colloids Surf., A* **2015**, *481* (Supplement C), 13–19.
- (99) Vodouhê, C.; Schmittbuhl, M.; Boulmedais, F.; Bagnard, D.; Vautier, D.; Schaaf, P.; Egles, C.; Voegel, J.-C.; Ogier, J. Effect of functionalization of multilayered polyelectrolyte films on motoneuron growth. *Biomaterials* **2005**, *26* (5), 545–554.
- (100) Lee, I. C.; Wu, Y. C. Assembly of polyelectrolyte multilayer films on supported lipid bilayers to induce neural stem/progenitor cell differentiation into functional neurons. *ACS Appl. Mater. Interfaces* **2014**, *6* (16), 14439–14450.
- (101) Gheith, M. K.; Sinani, V. A.; Wicksted, J. P.; Matts, R. L.; Kotov, N. A. Single-walled carbon nanotube polyelectrolyte multilayers and freestanding films as a biocompatible platform for neuroprosthetic implants. *Adv. Mater.* **2005**, *17* (22), 2663–2670.
- (102) Dierich, A.; Le Guen, E.; Messaddeq, N.; Stoltz, J. F.; Netter, P.; Schaaf, P.; Voegel, J. C.; Benkirane-Jessel, N. Bone formation mediated by synergy-acting growth factors embedded in a polyelectrolyte multilayer film. *Adv. Mater.* **2007**, *19* (5), 693–697.
- (103) Ren, Y. J.; Zhang, H.; Huang, H.; Wang, X. M.; Zhou, Z. Y.; Cui, F. Z.; An, Y. H. *In vitro* behavior of neural stem cells in response to different chemical functional groups. *Biomaterials* **2009**, *30* (6), 1036–1044.
- (104) Nolte, A. J.; Cohen, R. E.; Rubner, M. F. A two-plate buckling technique for thin film modulus measurements: applications to polyelectrolyte multilayers. *Macromolecules* **2006**, *39* (14), 4841–4847.
- (105) Yu, L. M. Y.; Leipzig, N. D.; Shoichet, M. S. Promoting neuron adhesion and growth-Review. *Mater. Today* **2008**, *11* (5), 36–43.
- (106) Schneider, A.; Francius, G.; Obeid, R.; Schwinte, P.; Hemmerle, J.; Frisch, B.; Schaaf, P.; Voegel, J. C.; Senger, B.; Picart, C. Polyelectrolyte multilayers with a tunable Young's modulus: influence of film stiffness on cell adhesion. *Langmuir* **2006**, *22* (3), 1193–1200.
- (107) He, W.; Bellamkonda, R. V. Nanoscale neuro-integrative coatings for neural implants. *Biomaterials* **2005**, *26* (16), 2983–2990.
- (108) Jan, E.; Hendricks, J. L.; Husaini, V.; Richardson-Burns, S. M.; Sereno, A.; Martin, D. C.; Kotov, N. A. Layered carbon nanotube-polyelectrolyte electrodes outperform traditional neural interface materials. *Nano Lett.* **2009**, *9* (12), 4012–4018.
- (109) Kidambi, S.; Lee, I.; Chan, C. Primary neuron/astrocyte coculture on polyelectrolyte multilayer films: a template for studying astrocyte-mediated oxidative stress in neurons. *Adv. Funct. Mater.* **2008**, *18* (2), 294–301.
- (110) Chluba, J.; Voegel, J.-C.; Decher, G.; Erbacher, P.; Schaaf, P.; Ogier, J. Peptide hormone covalently bound to polyelectrolytes and embedded into multilayer architectures conserving full biological activity. *Biomacromolecules* **2001**, *2* (3), 800–805.
- (111) Schmidt, D. J.; Moskowitz, J. S.; Hammond, P. T. Electrically triggered release of a small molecule drug from a polyelectrolyte multilayer coating. *Chem. Mater.* **2010**, *22* (23), 6416–6425.
- (112) Lei, K. F.; Lee, I. C.; Liu, Y. C.; Wu, Y. C. Successful differentiation of neural stem/progenitor cells cultured on electrically adjustable indium tin oxide (ITO) surface. *Langmuir* **2014**, *30* (47), 14241–14249.
- (113) Zhou, K.; Thouas, G. A.; Bernard, C. C.; Nisbet, D. R.; Finkelstein, D. I.; Li, D.; Forsythe, J. S. Method to impart electro- and biofunctionality to neural scaffolds using graphene-polyelectrolyte multilayers. *ACS Appl. Mater. Interfaces* **2012**, *4* (9), 4524–4531.
- (114) Cavelier, S.; Barrett, C. J.; Barthelat, F. The mechanical performance of a biomimetic nanointerface made of multilayered polyelectrolytes. *Eur. J. Inorg. Chem.* **2012**, *2012* (32), 5380–5389.
- (115) Mermut, O.; Lefebvre, J.; Gray, D. G.; Barrett, C. J. Structural and mechanical properties of polyelectrolyte multilayer films studied by AFM. *Macromolecules* **2003**, *36* (23), 8819–8824.
- (116) Burke, S. E.; Barrett, C. J. pH-responsive properties of multilayered poly(L-lysine)/hyaluronic acid surfaces. *Biomacromolecules* **2003**, *4* (6), 1773–1783.
- (117) Burke, S. E.; Barrett, C. J. Controlling the physicochemical properties of weak polyelectrolyte multilayer films through acid/base equilibria. *Pure Appl. Chem.* **2004**, *76* (7–8), 1387–1398.
- (118) Rodriguez, L.; De Paul, S.; Barrett, C. J.; Reven, L.; Spiess, H. W. Fast magic-angle spinning and double-quantum <sup>1</sup>H solid-state NMR spectroscopy of polyelectrolyte multilayers. *Adv. Mater.* **2000**, *12* (24), 1934–1938.
- (119) McCormick, M.; Smith, R.; Graf, R.; Barrett, C. J.; Reven, L.; Spiess, H. W. NMR studies of the effect of adsorbed water on polyelectrolyte multilayer films in the solid state. *Macromolecules* **2003**, *36* (10), 3616–3625.
- (120) Tanchak, O. M.; Barrett, C. J. Swelling dynamics of multilayer films of weak polyelectrolytes. *Chem. Mater.* **2004**, *16* (14), 2734–2739.

- (121) Burke, S. E.; Barrett, C. J. Swelling behavior of hyaluronic acid/polyallylamine hydrochloride multilayer films. *Biomacromolecules* **2005**, *6* (3), 1419–1428.
- (122) Harroun, T.; Fritzsche, H.; Watson, M.; Yager, K.; Tanchak, O.; Barrett, C. J.; Katsaras, J. Variable temperature, relative humidity (0%–100%), and liquid neutron reflectometry sample cell suitable for polymeric and biomimetic materials. *Rev. Sci. Instrum.* **2005**, *76* (6), 065101.
- (123) Tanchak, O. M.; Yager, K. G.; Fritzsche, H.; Harroun, T.; Katsaras, J.; Barrett, C. J. Ion distribution in multilayers of weak polyelectrolytes: A neutron reflectometry study. *J. Chem. Phys.* **2008**, *129* (8), 084901.
- (124) Ahmed, N. M.; Barrett, C. J. Novel azo chromophore-containing polymers: synthesis and characterization. *Polym. Mater. Sci. Eng.* **2001**, *85*, 607–608.
- (125) Schoelch, S.; Vapaavuori, J.; Rollet, F. G.; Barrett, C. J. The orange side of disperse red 1: humidity-driven color switching in supramolecular azo-polymer materials based on reversible dye aggregation. *Macromol. Rapid Commun.* **2017**, *38* (1), 1600582.
- (126) Goulet-Hanssens, A.; Barrett, C. J. Photo-control of biological systems with azobenzene polymers. *J. Polym. Sci., Part A: Polym. Chem.* **2013**, *51* (14), 3058–3070.
- (127) Goulet-Hanssens, A.; Lai Wing Sun, K.; Kennedy, T. E.; Barrett, C. J. Photoreversible surfaces to regulate cell adhesion. *Biomacromolecules* **2012**, *13* (9), 2958–2963.
- (128) Fernandez, R.; Ocando, C.; Fernandes, S. C.; Eceiza, A.; Tercjak, A. Optically active multilayer films based on chitosan and an azopolymer. *Biomacromolecules* **2014**, *15* (4), 1399–1407.
- (129) Sailer, M.; Fernandez, R.; Lu, X.; Barrett, C. J. High levels of molecular orientation of surface azo chromophores can be optically induced even in a wet biological environment. *Phys. Chem. Chem. Phys.* **2013**, *15* (46), 19985–19989.
- (130) Murphy, A. R.; St John, P.; Kaplan, D. L. Modification of silk fibroin using diazonium coupling chemistry and the effects on hMSC proliferation and differentiation. *Biomaterials* **2008**, *29* (19), 2829–2838.